Letter

Qubit decoherence under two-axis coupling to low-frequency noises

Guy Ramon [1,*] and Łukasz Cywiński [2,†]

[1] *Department of Physics, Santa Clara University, Santa Clara, California 95053, USA*

[2] *Institute of Physics, Polish Academy of Sciences, Aleja Lotnikow 32/46, PL-02668 Warsaw, Poland*

(Received 7 December 2021; accepted 21 January 2022; published 31 January 2022)

Many solid-state qubit systems are afflicted by low-frequency noise mechanisms that operate along two perpendicular axes of the Bloch sphere. Depending on the qubit control fields, either noise can be longitudinal or transverse to the quantization axis of the qubit, thus affecting its dynamics in distinct ways, generally contributing to decoherence that goes beyond pure dephasing. Here, we present a theory that provides a unified platform to study dynamics of a qubit subjected to two perpendicular low-frequency noises (assumed to be Gaussian and uncorrelated) under dynamical decoupling pulse sequences. The theory is demonstrated by the commonly encountered case of power law noise spectra, where approximate analytical results can be obtained.

DOI: 10.1103/PhysRevB.105.L041303

I. INTRODUCTION

Decoherence of qubits can be calculated relatively easily in two cases: that of pure dephasing due to Gaussian longitudinal noise acting along the energy quantization axis of the qubit [1,2] and that of Markovian evolution of open systems that applies when the relevant environmental fluctuations (coupled along any axis) act on timescales shorter than that of the open system dynamics of the qubit [3,4]. However, many solid-state qubits decohere due to environmental fluctuations with nonnegligible correlation times that couple along at least two perpendicular axes. Born-Markov treatment of both relaxation and dephasing is then inapplicable, and a general solution beyond the pure dephasing case is out of reach [5,6]. In the often-encountered case of noises with spectra concentrated at low frequencies—quasistatic or $1/f$ type [1]—an adiabatic treatment of qubit dynamics caused by multi-axis noise is possible [7,8]. Our focus here is on two-axis coupling of a qubit to such low-frequency noises, and we develop an approximate analytical solution to decoherence for a qubit that is freely evolving or subjected to dynamical decoupling (DD) sequences [2,9–14].

The Hamiltonian of the qubit-environment system can be written quite generally as

$$\mathcal{H}(t) = \tfrac{1}{2}[\mathbf{B} + \boldsymbol{\xi}(t)] \cdot \boldsymbol{\sigma}, \tag{1}$$

where $\mathbf{B}$ is a vector of the qubit control fields, $\boldsymbol{\xi}(t)$ is a vector of environmental quantum operators or classical stochastic functions representing noise, and $\boldsymbol{\sigma}$ is the vector of Pauli matrices. Strictly speaking, the qubit control fields are not static, as they typically include DD pulse sequences, but here, we assume instantaneous pulses that result in perfect π rotations of the qubit state around the y axis, perpendicular to both control and noise directions.

Solid-state devices are abundant with sources of low-frequency excitations such as slowly switching two-level fluctuators responsible for $1/f$ noise [1]. Prominent examples of solid-state-based qubits affected by two-axis low-frequency noise include those based on two [15–17] or three [18–22] exchange-coupled semiconductor quantum dots (QDs) containing at least two electrons and both charge and flux superconducting (SC) qubits [23–25]. In all these devices, electronic charge noise and flux noise spectra follow power law $1/f^{\alpha}$ over a wide range of frequencies, with α generally falling in the range of $\alpha = 1$–1.25 [26–30]. Several experiments reported other power laws, including $\alpha = 0.9$ for flux noise in a SC qubit [23], $\alpha = 0.7$ for charge noise in GaAs QDs [31], $\alpha = 1.93$ in a charge-tunable SC device inflicted with anomalous large-amplitude charge noise [32], and a dual power law of $\alpha = 1.48/1.97$ of charge noise in Si QD, where the higher power law was measured at extremely low frequencies $<10^{-4}$ Hz [33].

We focus here on the case of a two-electron singlet-triplet ($S - T_0$) qubit in a double QD (DQD), for which $\mathbf{B} = (\delta h, 0, J)$, where δh is the interdot magnetic field gradient across the QDs, and J is the exchange coupling [17,34]. The latter originates from Coulomb interaction and as such exhibits slow fluctuations [31,35–38] caused by $1/f^{\alpha}$ charge noise. Finite δh arises due to a spatially dependent field from a nanomagnet [33,39–41] or inhomogeneous nuclear spin polarization resulting in an Overhauser field gradient [42,43]. In the latter case, nuclear noise is concentrated at very low frequencies [44,45], and the quasistatic approximation breaks down only at timescales $>10\,\mu$s [46–48]. However, charge noise leads to stochastic shifts of the electron wave functions with respect to the frozen nuclei, thus making the Overhauser fields experienced by the electrons inherit the characteristics of charge noise [45,48]. The same happens when δh results from an external magnetic field gradient: charge noise induces variations in electron positions that translate into fluctuations of their spin splitting, thus δh. Consequently, noise in both δh and J is of $1/f^{\alpha}$ type at high frequencies, with an additional

*gramon@scu.edu

†lcyw@ifpan.edu.pl

zero-frequency component for δh accounting for nuclear spin diffusion. In GaAs QDs, δh noise power spectra characterized by $\alpha = 1$–2.6 were measured at frequencies between $\sim$1 kHz, below which classical nuclear spin diffusion results in a Lorentzian, quasistatic noise, and $\sim$100 kHz [44,45,49,50]. It should be stressed that our model for two low-frequency noises applies to all the abovementioned qubits, so while we present below results for the S-T_0 qubit, our theory applies to a wide class of systems.

Energy relaxation of the qubit depends on the availability of environmental excitations with appreciable transverse (with respect to the quantization axis set by **B**) coupling to the qubit and energy that is comparable with its level splitting. In contrast, environmental degrees of freedom with any energy contribute to pure dephasing of superpositions of the qubit eigenstates. In devices with strong low-frequency noises, the timescales of dephasing and relaxation are thus often well separated, with coherence becoming limited by relaxation only after application of a very large number of DD pulses [23]. This justifies our neglect of relaxation and focus on effects of dephasing and tilting of the quantization axis of the qubit. A crucial element of our theory follows from the fact that transverse noise couples to the qubit phase nonlinearly (quadratically in the lowest order). As a result, even a noise with Gaussian statistics becomes effectively non-Gaussian, and calculation of its higher-order cumulants, beyond the second one, is necessary to correctly evaluate the dephasing of the qubit [7,51–53].

In this paper, we develop a unified theory for the time evolution of a qubit state under two uncorrelated, zero-mean, low-frequency Gaussian noises that operate on perpendicular axes [54]. Our theory extends a previous analysis made by Barnes *et al.* [8] for S-T_0 qubits in two respects: (i) we perform the calculation to the second order in $\boldsymbol{\xi}(t)$, such that (quadratically coupled) transverse noise is considered, and (ii) we include DD control pulse sequences, accounting for qubit evolution outside the free induction decay (FID) case. The latter is made possible by the former, as effects of transverse noise are typically overshadowed by the longitudinal one when no DD filtering of the lowest-frequency longitudinal noise is done. We also include contributions resulting from the nontrivial interplay of longitudinal and transverse noises, as well as axis-tilting effects, thus providing a complete analytical treatment of the problem of decoherence due to two-axis slow noises.

II. FORMALISM

We specify the qubit working position for a two-axis control field $\mathbf{B} = (B_x, 0, B_z)$ using the angle $\overline{\chi} = \arctan(B_x/B_z)$, so that ξ_z, ξ_x in the Hamiltonian, Eq. (1), represent fluctuations of the respective control fields. We assume that these act on a much slower timescale, as compared with the qubit dynamics, allowing us to take the adiabatic limit, where the qubit evolution operator is approximated by applying instantaneous eigenstates of $\mathcal{H}(t)$ [8]. The resulting instantaneous unitary evolution reads

$$U(t) \approx \begin{pmatrix} \cos\phi - i\sin\phi\cos\chi & -i\sin\phi\sin\chi \\ -i\sin\phi\sin\chi & \cos\phi + i\sin\phi\cos\chi \end{pmatrix}, \tag{2}$$

where the noises impact the evolution by modifying the rotation axis $\chi(t)$ and the accumulated rotation angle $\phi(t)$:

$$\chi(t) = \arctan\left(\frac{B_x + \xi_x}{B_z + \xi_z}\right) \equiv \overline{\chi} + \delta\chi(t), \tag{3}$$

$$\phi(t) = \overline{\phi}(t) + \delta\phi(t). \tag{4}$$

Without noise, we have $\overline{\phi}(t) = \frac{1}{2}\int_0^t dt' f_t(t') B_z \sec\overline{\chi}$, where $f_t(t')$ is the switching function corresponding to the employed pulse protocol, whose Fourier transform $\tilde{f}_t(\omega)$ is known as the filter function [55]. For FID, $\overline{\phi}(t) = \sqrt{B_z^2 + B_x^2}\, t/2$, whereas any balanced pulse protocol yields $\overline{\phi}(t) = 0$ since $\int f_t(t')dt' = 0$. One can split the qubit-environment term in the Hamiltonian, Eq. (1), into parts that are parallel and perpendicular to the qubit control axis, using $\xi_\parallel = \xi_x \sin\overline{\chi} + \xi_z \cos\overline{\chi}$ and $\xi_\perp = \xi_x \cos\overline{\chi} - \xi_z \sin\overline{\chi}$. To second order in ξ_l, $l \in \{\parallel, \perp\}$, we have

$$\delta\chi(t) \approx \frac{\cos\overline{\chi}}{B_z}\xi_\perp(t)\left[1 - \frac{\cos\overline{\chi}}{B_z}\xi_\parallel(t)\right], \tag{5}$$

$$\delta\phi(t) \approx \frac{1}{2}\int_0^t dt' f_t(t')\left[\xi_\parallel(t') + \frac{\cos\overline{\chi}}{2B_z}\xi_\perp^2(t')\right]. \tag{6}$$

Utilizing the qubit Hamiltonian eigenstates in the tilted rotation axis $z' = (\sin\overline{\chi}, 0, \cos\overline{\chi})$:

$$|+\rangle = \begin{pmatrix} \cos\frac{\overline{\chi}}{2} \\ \sin\frac{\overline{\chi}}{2} \end{pmatrix}, \quad |-\rangle = \begin{pmatrix} -\sin\frac{\overline{\chi}}{2} \\ \cos\frac{\overline{\chi}}{2} \end{pmatrix}, \tag{7}$$

and the perpendicular state $|x'\rangle = \frac{1}{2}(|+\rangle + |-\rangle)$, the effects of the two noises can be quantified by the coherence function:

$$\begin{aligned} W(t) &= \frac{|\langle\rho_{+-}(t)\rangle|}{|\langle\rho_{+-}(0)\rangle|} = \left|\left\langle \frac{\langle +|U(t)|x'\rangle\langle x'|U^\dagger(t)|-\rangle}{\langle +|x'\rangle\langle x'|+\rangle}\right\rangle\right| \\ &= |\langle 1 - 2\sin\phi\cos\delta\chi(\cos\delta\chi\sin\phi + i\cos\phi)\rangle| \\ &\approx \left|e^{-2i\overline{\phi}}\langle e^{-2i\delta\phi}\rangle - \frac{1}{2}\langle\delta\chi^2(\cos 2\phi + e^{-2i\phi})\rangle\right|, \end{aligned} \tag{8}$$

where $\langle\cdot\rangle$ denotes Gaussian averaging over both ξ_z and ξ_x, and the last row is correct to the second order in these noises, with the first (second) term corresponding to the rotation angle (axis tilting) error.

The presence of quadratic noise terms in $\delta\phi$ requires a full cumulant expansion in the averaging since $\xi_l^2(t)$ are no longer Gaussian distributed [53]. For zero-mean Gaussian noises, $\langle\xi^k(t)\rangle = 0$ for odd k, and even-power terms factorize to two-point correlators $\langle\xi(t_1)\xi(t_2)\rangle \equiv S(t_{12})$, where $t_{12} \equiv t_1 - t_2$. Addressing first the dominant contribution due to rotation angle errors, we have

$$\langle e^{\pm 2i\delta\phi}\rangle = \exp\left\{\sum_{k=1}(\pm i)^k \frac{C_k}{k!}\right\}, \tag{9}$$

where C_k generalize the standard noise cumulants [56] for two uncorrelated noises and are given explicitly in terms of their noise power spectra in Sec. I of the Supplemental Material [57].

The structure of the kth cumulant reveals two types of contributions that we coin *linked* $R_k(t)$ (with k correlators) and *semilinked* $\tilde{R}_k(t)$ (with $k-1$ correlators):

$$R_k(t) = -\frac{1}{2k}\left(\frac{i}{B}\right)^k \int_0^\infty \frac{d\omega_1 \cdots d\omega_k}{\pi^k} \tilde{f}_t(\omega_{12}) \cdots \tilde{f}_t(\omega_{k1}) \times \prod_{i=1}^{k} [\sin^2 \overline{\chi} \tilde{S}_z(\omega_i) + \cos^2 \overline{\chi} \tilde{S}_x(\omega_i)], \tag{10}$$

$$\tilde{R}_k(t) = -\frac{1}{2}\left(\frac{i}{B}\right)^k (B_z \sin \overline{\chi})^2 \int_0^\infty \frac{d\omega_1 \cdots d\omega_{k-1}}{\pi^{k-1}} \times \tilde{f}_t(-\omega_1)[\tilde{S}_z(\omega_1) - \tilde{S}_x(\omega_1)]\tilde{f}_t(\omega_{12}) \times \prod_{i=2}^{k-2} \tilde{f}_t(\omega_{i,i+1})[\sin^2 \overline{\chi} \tilde{S}_z(\omega_i) + \cos^2 \overline{\chi} \tilde{S}_x(\omega_i)] \times \tilde{f}_t(\omega_{k-1})[\tilde{S}_z(\omega_{k-1}) - \tilde{S}_x(\omega_{k-1})]. \tag{11}$$

In Eqs. (10) and (11), $\tilde{S}_z(\omega)$ and $\tilde{S}_x(\omega)$ are the power spectra of the two noises. The linked diagrams involve only $\xi_\perp^2$ contributions, whereas the semilinked diagrams include a mixing of $\xi_\perp^2$ and $\xi_\parallel$ terms. Equation (9) then reads

$$\langle e^{\pm 2i\delta\phi} \rangle = c_z(t) c_x(t) \exp[-(\Sigma_{2k} + \tilde{\Sigma}_{2k})] \times \exp[\pm i(\Sigma_{2k+1} + \tilde{\Sigma}_{2k+1})], \tag{12}$$

where $\Sigma_{2k} \equiv \sum_{k=1} R_{2k}(t)$ $[\tilde{\Sigma}_{2k} \equiv \sum_{k=2} \tilde{R}_{2k}(t)]$ and $\Sigma_{2k+1} \equiv i \sum_{k=0} R_{2k+1}(t)$ $[\tilde{\Sigma}_{2k+1} \equiv i \sum_{k=1} \tilde{R}_{2k+1}(t)]$ are the summations over linked (semilinked) even and odd diagrams, respectively, and we singled out the semilinked contributions in the second cumulant that are accounted for in Ref. [8]:

$$c_z(t) = \exp\left\{-\cos^2 \overline{\chi} \int_0^\infty \frac{d\omega}{2\pi} |\tilde{f}_t(\omega)|^2 \tilde{S}_z(\omega)\right\},$$
$$c_x(t) = \exp\left\{-\sin^2 \overline{\chi} \int_0^\infty \frac{d\omega}{2\pi} |\tilde{f}_t(\omega)|^2 \tilde{S}_x(\omega)\right\}. \tag{13}$$

For an odd number of DD pulses, $\tilde{f}_t(\omega)$ is an odd function, and only even cumulants survive. In this case, the phase terms in Eq. (12) vanish, and only signal decay remains.

The evaluation of the axis-error, transient contribution in Eq. (8) is more involved, and the calculational details can be found in Sec. II of the Supplemental Material [57]. We note here that the leading terms in this contribution vanish for any balanced DD pulse sequence. Finally, we provide for completeness formulas for singlet and $|\uparrow\downarrow\rangle$ return probabilities, correct to the second order in noise amplitudes, under any DD pulse sequence [57], corresponding to experiments reported in Refs. [45,58], respectively.

III. CUMULANT RESUMMATION FOR LOW-FREQUENCY NOISES

We use the resummation technique of Ref. [53] to derive analytical results for the cumulant sums found in the rotation angle error contribution, Eq. (12), and for the various time derivatives of these sums in the axis-error contribution [57]. We split the noise into a dominant low-frequency, static component and a high-frequency, time-dependent component $\xi_l = \xi_l^{\rm lf} + \xi_l^{\rm hf}(t)$ and denote the standard deviations of the low- and high-frequency noise components as

$$\sigma_{0l}^2 = \int_{\omega_0}^{\omega_1} \frac{d\omega}{\pi} \tilde{S}_l(\omega), \quad \sigma_{tl}^2 = \int_{\omega_1}^{\infty} \frac{d\omega}{\pi} \tilde{S}_l(\omega), \tag{14}$$

where ω_0 is a low-frequency cutoff, determined by the shorter of the noise correlation time and the total acquisition time, both of which are typically much longer than t, and ω_1 can be taken as $1/t$ or otherwise as a fixed ultraviolet cutoff. Our approximate calculation of the cumulant sums rests on the assumption that $\sigma_{tl}^2 \ll \sigma_{0l}^2$ for both noises at timescales relevant for the qubit operation. This assumption holds for any power law noise with $\alpha \geqslant 1$.

Replacing each noise correlator with $S_l(t_{ij}) = \langle \xi_l^{\rm hf}(t_i) \xi_l^{\rm hf}(t_j) \rangle_{\rm hf} + \sigma_{0l}^2$ and keeping only terms with maximal power of σ_{0l}^2, we derive explicit expressions for the cumulant terms and their time derivatives [57] and perform the summations in Eq. (12). Whereas for any balanced DD sequence this procedure amounts to replacing every second correlator with σ_{0l}^2, in the FID case, *all* correlators are replaced with σ_{0l}^2. The linked and semilinked even sums are found respectively as

$$\exp(-\Sigma_{2k}) = \begin{cases} \sqrt{\eta(t)}, & \text{DD} \\ \eta_{\rm FID}^{1/4}(t), & \text{FID} \end{cases}, \tag{15}$$

and

$$\tilde{\Sigma}_{2k} = \begin{cases} \frac{\eta(t)}{2}\left(\frac{B_x B_z}{B^3}\right)^2 \left[\tilde{f}_t^2(0) \overline{S}_+^{\rm hf}(t) \sigma_{0-}^4 + [S_-^{\rm hf}(t)]^2 \overline{\sigma}_{0+}^2\right], & \text{DD} \\ \frac{\eta_{\rm FID}(t)}{2}\left(\frac{B_x B_z}{B^3}\right)^2 \sigma_{0-}^4 \overline{\sigma}_{0+}^2 t^4, & \text{FID} \end{cases}, \tag{16}$$

where we have defined

$$\eta(t) \equiv \left[1 + \frac{\overline{\sigma}_{0+}^2 \overline{S}_+^{\rm hf}(t)}{B^2}\right]^{-1}; \quad \eta_{\rm FID}(t) \equiv \left(1 + \frac{\overline{\sigma}_{0+}^4 t^2}{B^2}\right)^{-1}. \tag{17}$$

In Eqs. (16) and (17), $\sigma_{0\pm}^2 \equiv \sigma_{0z}^2 \pm \sigma_{0x}^2$, $\overline{\sigma}_{0\pm}^2 \equiv \sin^2 \overline{\chi} \sigma_{0z}^2 \pm \cos^2 \overline{\chi} \sigma_{0x}^2$, and similarly, the high-frequency combined noise correlators are given by $S_\pm^{\rm hf}(t) = S_z^{\rm hf}(t) \pm S_x^{\rm hf}(t)$, $\overline{S}_\pm^{\rm hf}(t) = \sin^2 \overline{\chi} S_z^{\rm hf}(t) \pm \cos^2 \overline{\chi} S_x^{\rm hf}(t)$, where $S_l^{\rm hf}(t) = \int_{\omega_1}^\infty \frac{d\omega}{\pi} |\tilde{f}_t(\omega)|^2 \tilde{S}_l(\omega)$. The sums over odd diagrams in Eq. (12) are nonzero only for FID, giving a nontrivial phase shift in $W(t)$ that is characteristic for free evolution dephasing due to low-frequency transverse noise [7,59,60]:

$$\Sigma_{2k+1}^{\rm FID}(t) = \frac{1}{2} \arctan\left(\frac{\overline{\sigma}_{0+}^2 t}{B}\right),$$
$$\tilde{\Sigma}_{2k+1}^{\rm FID}(t) = -\frac{\sin^2 2\overline{\chi}}{8B} \eta_{\rm FID}(t) \sigma_{0-}^4 t^3. \tag{18}$$

We calculated the highest subleading contribution due to linked odd diagrams with one less σ_{0l}^2 factor, showing it to be negligible for experimentally relevant noise parameters [57].

IV. RESULTS

We now demonstrate the versatility of our two-axis noise theory in predicting decoherence at arbitrary working positions by considering real-life noise parameters pertaining to

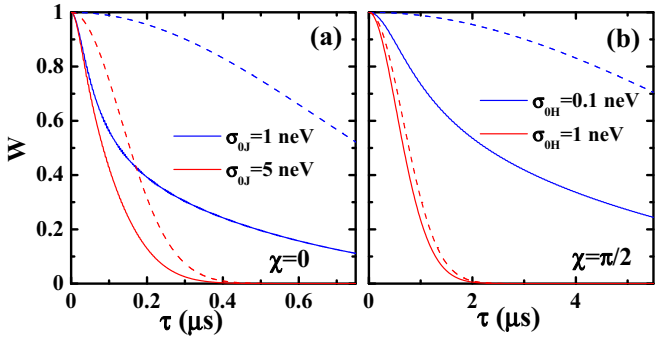

FIG. 1. FID decoherence function, Eq. (8), calculated to the first order (dashed lines) and with a full cumulant summation (solid lines). (a) $J = 0.5\ \mu$eV, $\delta h = 0$ ($\overline{\chi} = 0$), $\sigma_{0H} = 0.1\,\mu$eV relevant for GaAs QDs, $\sigma_{0J} = 1$ neV (blue lines) and 5 neV (red Lines), and $A_J = \sigma_{0J}/5$. The perpendicular noise contribution becomes dominant with smaller charge noise amplitudes. (b) $J = 0$, $\delta h = 0.1\,\mu$eV ($\overline{\chi} = \pi/2$), $\sigma_{0J} = 10$ neV, and $A_J = 0.2\sigma_{0J}$. We consider low static magnetic noise values $\sigma_{0H} = 1$ and 0.1 neV with the latter relevant for isotopically purified Si QDs with micromagnets [33,40].

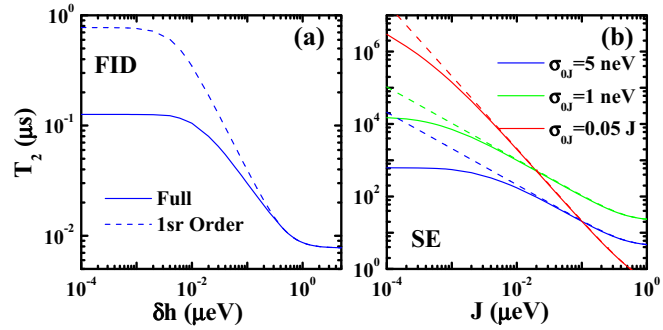

FIG. 2. Dephasing times for quasistatic nuclear noise ($\sigma_{0H} = 0.1\,\mu$eV, $A_H = 0$) as a function of (a) δh for FID at $J = 0.5\,\mu$eV, $\sigma_{0J} = 1$ neV and (b) J for spin echo (SE) at $\delta h = 0.5\ \mu$eV. Several charge noise models are shown in (b), including $\sigma_{0J} = 5$ neV (red), 1 neV (green), and $0.05J$ (blue). Solid lines depict full cumulant summation, and dashed lines show first-order calculation. In all cases, $A_J = \sigma_{0J}/5$.

the charge (J) and magnetic (H) control fields in singlet-triplet spin qubits. We consider $\alpha_J = \alpha_H = 1$, such that $\tilde{S}_{J/H} = A^2_{J/H}/\omega$ for both noise spectra with a low-frequency cutoff of $\omega_0 = 1$ Hz, and include for the nuclear noise a quasistatic contribution $S^{qs}_H = \sigma^2_{0H}\delta(\omega)$. Unless otherwise noted, we take the high-frequency nuclear noise amplitude as $A_H = 66$ peV [50], attributed to shaking of the electronic wave function by charge noise. For $\alpha_J = 1$, we have $A_J \approx \sigma_{0J}/5$ at typical ω_0 values and $A_J \approx 10^{-3}J$, as was measured in Ref. [31].

In Figs. 1(a) and 1(b), we consider FID at $\overline{\chi} = 0$ and $\pi/2$, respectively, focusing on scenarios where the transverse ($\perp$) noise contribution is comparable or greater than the longitudinal ($\parallel$) one. In either case, the main contribution to the longitudinal noise comes from $c_{x/z}$, Eq. (13), resulting in dephasing time of $T_{2\parallel} = \sqrt{2}/\sigma_{0\parallel}$, whereas the dominant contribution to the transverse noise comes from the linked terms, Eqs. (15) and (17), resulting in dephasing time of $T_{2\perp} \approx 7.3B_\parallel/\sigma^2_{0\perp}$ [61]. For $\overline{\chi} = 0$, the transverse (nuclear) noise contribution can easily dominate dephasing due to the relatively large Overhauser field gradient static noise of $\sigma_{0H} = 0.1\ \mu$eV, measured for GaAs QDs [50] [see Fig. 1(a)], but at $\overline{\chi} = \pi/2$ [Fig. 1(b)], the transverse (charge) noise contribution becomes important only for a quiet magnetic environment, e.g., by implementing a field gradient with local micromagnets ($\sigma_{0H} \lesssim 0.1$ neV was measured in isotopically purified Si QDs with nanomagnets and charge noise dominating spin dephasing [33,40]). As the quantization axis tilts $\overline{\chi} \gtrsim 0$, the longitudinal noise contribution includes a nuclear noise component, thus becoming dominant with a resulting Gaussian decay. This is demonstrated in Fig. 2(a), where we provide T_2 FID times vs δh for $J = 0.5\,\mu$eV. With increasing δh, decay is dominated by longitudinal contribution, adequately described by the first-order calculation.

To provide an intuitive explanation for the decoherence in a DD setting, we consider spin echo (SE) as an example, assume quasistatic nuclear noise ($A_H = 0$), and again limit our discussion to the linked terms, Eqs. (15) and (17) (this picture is largely unchanged if small dynamic nuclear noise is added). Starting at $\overline{\chi} = 0$, we have Gaussian decay due to longitudinal noise $T^{\rm DD}_{2J} \approx 3/A_J$, while the quasistatic transverse noise is echoed away. As $\overline{\chi}$ increases, the longitudinal dephasing time becomes $T^{\rm DD}_{2\parallel} = T^{\rm DD}_{2J}/\cos\overline{\chi}$, whereas under the reasonable assumptions $A_J \gg A_H$, $\sigma_{0J} \ll \sigma_{0H}$, Eq. (17) gives $T^{\rm DD}_{2\perp} \approx 2BT^{\rm DD}_{2J}/(\sigma_{0H}\sin 2\overline{\chi})$ as long as $\tan\overline{\chi} \ll \sigma_{0H}/\sigma_{0J}$ is met. As $\overline{\chi}$ approaches $\pi/2$, longitudinal noise becomes irrelevant, whereas the transverse dephasing time saturates at $T^{\rm DD}_{2\perp} \approx BT^{\rm DD}_{2J}/\sigma_{0J}$. Figure 2(b) illustrates this nontrivial two-axis behavior, showing a crossover from the power law to Gaussian decay for SE.

Finally, Eq. (17) suggests that the transverse dynamic noise contribution is renormalized by $\overline{\sigma}^2_{0+}$, resulting in an unexpected effect whereby longitudinal quasistatic noise can impact decoherence under DD. This effect is demonstrated in Fig. 3, where we consider $\delta h \gg J$ and show that increas-

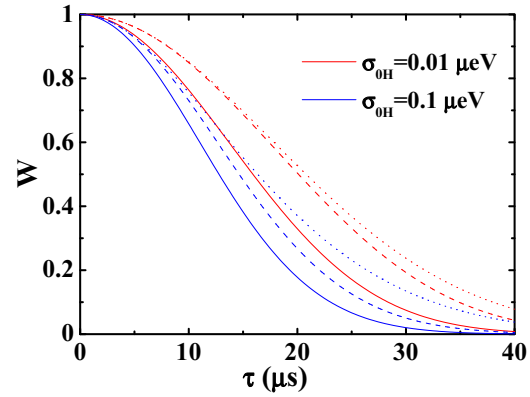

FIG. 3. Decoherence function vs time for SE at $\delta h = 0.1\,\mu$eV, $J = 0.02\,\mu$eV. The charge noise parameters are $\sigma_{0J} = 5$ neV and $A_J = \sigma_{0J}/5$, and we compare nuclear quasistatic noise of $\sigma_{0H} = 0.01\ \mu$eV (dashed red) and $0.1\ \mu$eV (dashed blue). Solid lines depict decoherence with additional dynamic nuclear noise with amplitude $A_H = 66$ peV. Dotted lines illustrate the results for $A_H = 0$ excluding the semilinked contribution from Eq. (16).

ing the (predominantly) longitudinal nuclear quasistatic noise from $\sigma_{0H} = 0.01$ to 0.1 μeV results in 25% (37%) reduction in dephasing time with (without) additional dynamic noise. We note that additional longitudinal-transverse noise mixing originates from the semilinked contributions, as seen by comparing dashed lines (full calculation) with dotted lines (excluding semilinked terms) in Fig. 3.

V. CONCLUSIONS

We have developed a theory to evaluate qubit state evolution under two perpendicular low-frequency noises and obtained closed-form results for the decoherence in both FID and DD settings by utilizing cumulant summations. Our theory captures the dynamics of the qubit at any working point, including the optimal point, where transverse noise (missing in previous first-order treatments) dominates and, near that point, where the interplay between longitudinal and transverse noises leads to nontrivial dynamics.

ACKNOWLEDGMENTS

G.R. wishes to thank Yonatan Ramon for working out elements of the calculations detailed in Sec. IV of the Supplemental Material [57]. This paper was supported by the National Science Foundation Grant No. DMR 1829430.

[1] E. Paladino, Y. M. Galperin, G. Falci, and B. L. Altshuler, $1/f$ noise: Implications for solid-state quantum information, Rev. Mod. Phys. **86**, 361 (2014).

[2] P. Szańkowski, G. Ramon, J. Krzywda, D. Kwiatkowski, and Ł. Cywiński, Environmental noise spectroscopy with qubits subjected to dynamical decoupling, J. Phys.: Condens. Matter **29**, 333001 (2017).

[3] H. Breuer and F. Petruccione, *The Theory of Open Quantum Systems* (Oxford University Press, Oxford, 2007).

[4] Á. Rivas and S. F. Huelga, *Open Quantum Systems* (Springer, Heidelberg, 2012).

[5] M. Aihara, H. M. Sevian, and J. L. Skinner, Non-markovian relaxation of a spin-$\frac{1}{2}$ particle in a fluctuating transverse field: cumulant expansion and stochastic simulation results, Phys. Rev. A **41**, 6596 (1990).

[6] H. Risken, L. Schoendorff, and K. Vogel, Relaxation of a spin-$\frac{1}{2}$ particle driven by transverse colored gaussian noise: Time dependence and eigenvalues, Phys. Rev. A **42**, 4562 (1990).

[7] G. Falci, A. D'Arrigo, A. Mastellone, and E. Paladino, Initial Decoherence in Solid State Qubits, Phys. Rev. Lett. **94**, 167002 (2005).

[8] E. Barnes, M. S. Rudner, F. Martins, F. K. Malinowski, C. M. Marcus, and F. Kuemmeth, Filter function formalism beyond pure dephasing and non-Markovian noise in singlet-triplet qubits, Phys. Rev. B **93**, 121407(R) (2016).

[9] L. Viola, E. Knill, and S. Lloyd, Dynamical Decoupling of Open Quantum Systems, Phys. Rev. Lett. **82**, 2417 (1999).

[10] A. G. Kofman and G. Kurizki, Unified Theory of Dynamically Suppressed Qubit Decoherence in Thermal Baths, Phys. Rev. Lett. **93**, 130406 (2004).

[11] M. J. Biercuk, A. C. Doherty, and H. Uys, Dynamical decoupling sequence construction as a filter-design problem, J. Phys. B: At. Mol. Opt. Phys. **44**, 154002 (2011).

[12] D. A. Lidar, Review of decoherence-free subspaces, noiseless subsystems, and dynamical decoupling, Adv. Chem. Phys. **154**, 295 (2014).

[13] D. Suter and G. A. Álvarez, Colloquium: Protecting quantum information against environmental noise, Rev. Mod. Phys. **88**, 041001 (2016).

[14] C. L. Degen, F. Reinhard, and P. Cappellaro, Quantum sensing, Rev. Mod. Phys. **89**, 035002 (2017).

[15] J. R. Petta, A. C. Johnson, J. M. Taylor, E. A. Laird, A. Yacoby, M. D. Lukin, C. M. Marcus, M. P. Hanson, and A. C. Gossard, Coherent manipulation of coupled electron spins in semiconductor quantum dots, Science **309**, 2180 (2005).

[16] J. M. Taylor, H. Engel, W. Dür, A. Yacoby, C. M. Marcus, P. Zoller, and M. D. Lukin, Fault-tolerant architecture for quantum computation using electrically controlled semiconductor spins, Nat. Phys. **1**, 177 (2005).

[17] J. M. Taylor, J. R. Petta, A. C. Johnson, A. Yacoby, C. M. Marcus, and M. D. Lukin, Relaxation, dephasing, and quantum control of electron spins in double quantum dots, Phys. Rev. B **76**, 035315 (2007).

[18] J. Medford, J. Beil, J. M. Taylor, E. I. Rashba, H. Lu, A. C. Gossard, and C. M. Marcus, Quantum-Dot-Based Resonant Exchange Qubit, Phys. Rev. Lett. **111**, 050501 (2013).

[19] J. Medford, J. Beil, J. M. Taylor, S. D. Bartlett, A. C. Doherty, E. I. Rashba, D. P. DiVincenzo, H. Lu, A. C. Gossard, and C. M. Marcus, Self-consistent measurement and state tomography of an exchange-only spin qubit, Nat. Nanotechnol. **8**, 654 (2013).

[20] M. Russ, F. Ginzel, and G. Burkard, Coupling of three-spin qubits to their electric environment, Phys. Rev. B **94**, 165411 (2016).

[21] A. Sala and J. Danon, Exchange-only singlet-only spin qubit, Phys. Rev. B **95**, 241303(R) (2017).

[22] M. Russ, J. R. Petta, and G. Burkard, Quadrupolar Exchange-Only Spin Qubit, Phys. Rev. Lett. **121**, 177701 (2018).

[23] J. Bylander, S. Gustavsson, F. Yan, F. Yoshihara, K. Harrabi, G. Fitch, D. G. Cory, Y. Nakamura, J.-S. Tsai, and W. D. Oliver, Noise spectroscopy through dynamical decoupling with a superconducting flux qubit, Nat. Phys. **7**, 565 (2011).

[24] F. Yan, S. Gustavsson, A. Kamal, J. Birenbaum, A. P. Sears, D. Hover, T. J. Gudmundsen, D. Rosenberg, G. Samach, S. Weber, J. L. Yoder, T. P. Orlando, J. Clarke, A. J. Kerman, and W. D. Oliver, The flux qubit revisited to enhance coherence and reproducibility, Nat. Commun. **7**, 12964 (2016).

[25] P. Krantz, M. Kjaergaard, F. Yan, T. P. Orlando, S. Gustavsson, and W. D. Oliver, A quantum engineer's guide to superconducting qubits, Appl. Phys. Rev. **6**, 021318 (2019).

[26] Y. Nakamura, Y. A. Pashkin, T. Yamamoto, and J. S. Tsai, Charge Echo in a Cooper-Pair Box, Phys. Rev. Lett. **88**, 047901 (2002).

[27] O. Astafiev, Y. A. Pashkin, Y. Nakamura, T. Yamamoto, and J. S. Tsai, Quantum Noise in the Josephson Charge Qubit, Phys. Rev. Lett. **93**, 267007 (2004).

[28] S. W. Jung, T. Fujisawa, Y. Hirayama, and Y. H. Jeong, Back-

ground charge fluctuation in a GaAs quantum dot device, Appl. Phys. Lett. **85**, 768 (2004).
[29] M. V. Gustafsson, A. Pourkabirian, G. Johansson, J. Clarke, and P. Delsing, Thermal properties of charge noise sources, Phys. Rev. B **88**, 245410 (2013).
[30] J. S. S. Blake M. Freeman and H. W. Jiang, Comparison of low frequency charge noise in identically patterned Si/SiO_2 and Si/SiGe quantum dots, Appl. Phys. Lett. **108**, 253108 (2016).
[31] O. E. Dial, M. D. Shulman, S. P. Harvey, H. Bluhm, V. Umansky, and A. Yacoby, Charge Noise Spectroscopy Using Coherent Exchange Oscillations in a Singlet-Triplet Qubit, Phys. Rev. Lett. **110**, 146804 (2013).
[32] B. G. Christensen, C. D. Wilen, A. Opremcak, J. Nelson, F. Schlenker, C. H. Zimonick, L. Faoro, L. B. Ioffe, Y. J. Rosen, J. L. DuBois, B. L. T. Plourde, and R. McDermott, Anomalous charge noise in superconducting qubits, Phys. Rev. B **100**, 140503(R) (2019).
[33] T. Struck, A. Hollmann, F. Schauer, O. Fedorets, A. Schmidbauer, K. Sawano, H. Riemann, N. V. Abrosimov, Ł. Cywiński, D. Bougeard, and L. R. Schreiber, Low-frequency spin qubit detuning noise in highly purified ^{28}Si/SiGe, npj Quantum Inf. **6**, 40 (2020).
[34] W. A. Coish and D. Loss, Singlet-triplet decoherence due to nuclear spins in a double quantum dot, Phys. Rev. B **72**, 125337 (2005).
[35] X. Hu and S. Das Sarma, Charge-Fluctuation-Induced Dephasing of Exchange-Coupled Spin Qubits, Phys. Rev. Lett. **96**, 100501 (2006).
[36] D. Culcer, X. Hu, and S. D. Sarma, Dephasing of Si spin qubits due to charge noise, Appl. Phys. Lett. **95**, 073102 (2009).
[37] G. Ramon and X. Hu, Decoherence of spin qubits due to a nearby charge fluctuator in gate-defined double dots, Phys. Rev. B **81**, 045304 (2010).
[38] G. Ramon, Dynamical decoupling of a singlet-triplet qubit afflicted by a charge fluctuator, Phys. Rev. B **86**, 125317 (2012).
[39] R. Brunner, Y.-S. Shin, T. Obata, M. Pioro-Ladrière, T. Kubo, K. Yoshida, T. Taniyama, Y. Tokura, and S. Tarucha, Two-Qubit Gate of Combined Single-Spin Rotation and Interdot Spin Exchange in a Double Quantum Dot, Phys. Rev. Lett. **107**, 146801 (2011).
[40] J. Yoneda, K. Takeda, T. Otsuka, T. Nakajima, M. R. Delbecq, G. Allison, T. Honda, T. Kodera, S. Oda, Y. Hoshi, N. Usami, K. M. Itoh, and S. Tarucha, A quantum-dot spin qubit with coherence limited by charge noise and fidelity higher than 99.9%, Nat. Nanotechnol. **13**, 102 (2018).
[41] D. M. Zajac, A. J. Sigillito, M. Russ, F. Borjans, J. M. Taylor, G. Burkard, and J. R. Petta, Resonantly driven CNOT gate for electron spins, Science **359**, 439 (2018).
[42] S. Foletti, H. Bluhm, D. Mahalu, V. Umansky, and A. Yacoby, Universal quantum control of two-electron spin quantum bits using dynamic nuclear polarization, Nat. Phys. **5**, 903 (2009).
[43] H. Bluhm, S. Foletti, D. Mahalu, V. Umansky, and A. Yacoby, Enhancing the Coherence of a Spin Qubit by Operating it as a Feedback Loop That Controls its Nuclear Spin Bath, Phys. Rev. Lett. **105**, 216803 (2010).
[44] D. J. Reilly, J. M. Taylor, E. A. Laird, J. R. Petta, C. M. Marcus, M. P. Hanson, and A. C. Gossard, Measurement of Temporal Correlations of the Overhauser Field in a Double Quantum Dot, Phys. Rev. Lett. **101**, 236803 (2008).
[45] F. K. Malinowski, F. Martins, Ł. Cywiński, M. S. Rudner, P. D. Nissen, S. Fallahi, G. C. Gardner, M. J. Manfra, C. M. Marcus, and F. Kuemmeth, Spectrum of the Nuclear Environment for GaAs Spin Qubits, Phys. Rev. Lett. **118**, 177702 (2017).
[46] W. M. Witzel and S. Das Sarma, Quantum theory for electron spin decoherence induced by nuclear spin dynamics in semiconductor quantum computer architectures: spectral diffusion of localized electron spins in the nuclear solid-state environment, Phys. Rev. B **74**, 035322 (2006).
[47] W. M. Witzel and S. Das Sarma, Multiple-Pulse Coherence Enhancement of Solid State Spin Qubits, Phys. Rev. Lett. **98**, 077601 (2007).
[48] H. Bluhm, S. Foletti, I. Neder, M. Rudner, D. Mahalu, V. Umansky, and A. Yacoby, Dephasing time of GaAs electron-spin qubits coupled to a nuclear bath exceeding 200 μs, Nat. Phys. **7**, 109 (2011).
[49] J. Medford, Ł. Cywiński, C. Barthel, C. M. Marcus, M. P. Hanson, and A. C. Gossard, Scaling of Dynamical Decoupling for Spin Qubits, Phys. Rev. Lett. **108**, 086802 (2012).
[50] F. K. Malinowski, F. Martins, P. D. Nissen, E. Barnes, Ł. Cywiński, M. S. Rudner, S. Fallahi, G. C. Gardner, M. J. Manfra, C. M. Marcus, and F. Kuemmeth, Notch filtering the nuclear environment of a spin qubit, Nat. Nanotechnol. **12**, 16 (2017).
[51] Y. Makhlin and A. Shnirman, Dephasing of Solid-State Qubits at Optimal Points, Phys. Rev. Lett. **92**, 178301 (2004).
[52] J. Bergli, Y. M. Galperin, and B. L. Altshuler, Decoherence of a qubit by a non-Gaussian noise at an arbitrary working point, Phys. Rev. B **74**, 024509 (2006).
[53] Ł. Cywiński, Dynamical-decoupling noise spectroscopy at an optimal working point of a qubit, Phys. Rev. A **90**, 042307 (2014).
[54] While the high-frequency noise component in δh is likely the result of charge noise, it is still reasonable to assume that the two noises are only weakly correlated, as detuning is mostly sensitive to the electric field along the axis connecting the two dots, while the Overhauser fields are sensitive to all components of the noisy electric fields.
[55] Ł. Cywiński, R. M. Lutchyn, C. P. Nave, and S. Das Sarma, How to enhance dephasing time in superconducting qubits, Phys. Rev. B **77**, 174509 (2008).
[56] R. Kubo, Generalized cumulant expansion method, J. Phys. Soc. Jpn. **17**, 1100 (1962).
[57] See Supplemental Material at http://link.aps.org/supplemental/10.1103/PhysRevB.105.L041303 for additional details on noise cumulants, axis-error contributions, and cumulant resummations.
[58] F. Martins, F. K. Malinowski, P. D. Nissen, E. Barnes, S. Fallahi, G. C. Gardner, M. J. Manfra, C. M. Marcus, and F. Kuemmeth, Noise Suppression Using Symmetric Exchange Gates in Spin Qubits, Phys. Rev. Lett. **116**, 116801 (2016).
[59] F. H. L. Koppens, D. Klauser, W. A. Coish, K. C. Nowack, L. P. Kouwenhoven, D. Loss, and L. M. K. Vandersypen, Universal Phase Shift and Nonexponential Decay of Driven Single-Spin Oscillations, Phys. Rev. Lett. **99**, 106803 (2007).
[60] Ł. Cywiński, W. M. Witzel, and S. Das Sarma, Pure quantum dephasing of a solid-state electron spin qubit in a large nuclear spin bath coupled by long-range hyperfine-mediated interaction, Phys. Rev. B **79**, 245314 (2009).
[61] Note that semilinked terms contribution, Eq. (16), can be substantial, providing additional weight to the perpendicular noise.

Supplemental Material for "Qubit Decoherence under two-axis coupling to low-frequency noises"

Guy Ramon[1,*] and Łukasz Cywiński[2,†]

[1]*Department of Physics, Santa Clara University, Santa Clara, CA 95053*
[2]*Institute of Physics, Polish Academy of Sciences, Aleja Lotnikow 32/46, PL-02668 Warsaw, Poland*

I. CUMULANTS FOR TWO PERPENDICULAR NON-CORRELATED NOISES

Starting with Eq. (6) in the main text, we perform Gaussian averaging of $2\delta\phi$ over both ξ_x and ξ_z. Assuming zero-mean noises, we keep only terms with even powers of either ξ_l, and find the first few cumulants of the combined two noises as:

$$C_1 = \langle 2\delta\phi\rangle = \frac{\cos\overline{\chi}}{2B_z}\left[\sin^2\overline{\chi}S_z(0)+\cos^2\overline{\chi}S_x(0)\right]\int dt_1 f_t(t_1) \tag{I.1}$$

$$C_2 = \langle(2\delta\phi)^2\rangle - \langle 2\delta\phi\rangle^2 = \int dt_1 dt_2 f_t(t_1)f_t(t_2)\Big\{\frac{\cos^2\overline{\chi}}{2B_z^2}\left[\sin^2\overline{\chi}S_z(t_{12})+\cos^2\overline{\chi}S_x(t_{12})\right]\left[\sin^2\overline{\chi}S_z(t_{21})+\cos^2\overline{\chi}S_x(t_{21})\right]+$$
$$\left[\cos^2\overline{\chi}S_z(t_{12})+\sin^2\overline{\chi}S_x(t_{12})\right]\Big\} \tag{I.2}$$

$$C_3 = \langle(2\delta\phi)^3\rangle - 3\langle(2\delta\phi)^2\rangle\langle 2\delta\phi\rangle + 2\langle 2\delta\phi\rangle^3 = \int dt_1 dt_2 dt_3 f_t(t_1)f_t(t_2)f_t(t_3)$$
$$\left\{\frac{\cos^3\overline{\chi}}{B_z^3}\prod_{\substack{i=1\\(k+1=1)}}^{k=3}\left[\sin^2\overline{\chi}S_z(t_{i,i+1})+\cos^2\overline{\chi}S_x(t_{i,i+1})\right]+\frac{3}{B_z}\cos^3\overline{\chi}\sin^2\overline{\chi}\left[S_z(t_{13})-S_x(t_{13})\right]\left[S_z(t_{23})-S_x(t_{23})\right]\right\} \tag{I.3}$$

$$C_4 = \langle(2\delta\phi)^4\rangle - 4\langle(2\delta\phi)^3\rangle\langle 2\delta\phi\rangle - 3\langle(2\delta\phi)^2\rangle^2 + 12\langle(2\delta\phi)^2\rangle\langle 2\delta\phi\rangle^2 - 6\langle 2\delta\phi\rangle^4 = \int dt_1\cdots dt_4 f_t(t_1)\cdots f_t(t_4)$$
$$\Big\{\frac{3\cos^4\overline{\chi}}{B_z^4}\prod_{\substack{i=1\\(k+1\to 1)}}^{k=4}\left[\sin^2\overline{\chi}S_z(t_{i,i+1})+\cos^2\overline{\chi}S_x(t_{i,i+1})\right]+\frac{12}{B_z^2}\cos^4\overline{\chi}\sin^2\overline{\chi}\left[S_z(t_{12})-S_x(t_{12})\right]\times$$
$$\left[\sin^2\overline{\chi}S_z(t_{23})+\cos^2\overline{\chi}S_x(t_{23})\right]\left[S_z(t_{34})-S_x(t_{34})\right]\Big\}. \tag{I.4}$$

We note that the last term in C_2 results in the rotation angle error contribution found in [1], whereas all other terms and cumulants are absent in the first-order calculation.

In terms of the noise power spectra and the Fourier transformed filter functions:

$$\tilde{S}_l(\omega) = \int_{-\infty}^{\infty} e^{i\omega t}S_l(t)dt, \tag{I.5}$$

$$\tilde{f}_t(\omega) = \int_{-\infty}^{\infty} e^{i\omega t'}f_t(t')dt', \tag{I.6}$$

the kth cumulant (for $k\geq 3$) is found as:

$$C_k = \frac{(k-1)!}{2}\left(\frac{\cos\overline{\chi}}{B_z}\right)^k\int_0^{\infty}\frac{d\omega_1\cdots d\omega_k}{\pi^k}\tilde{f}_t(\omega_{12})\cdots\tilde{f}_t(\omega_{k1})\prod_{i=1}^{k}\left[\sin^2\overline{\chi}\tilde{S}_z(\omega_i)+\cos^2\overline{\chi}\tilde{S}_x(\omega_i)\right]+\frac{k!}{8}\left(\frac{\cos\overline{\chi}}{B_z}\right)^{k-2}$$
$$\sin^2 2\overline{\chi}\int_0^{\infty}\frac{d\omega_1\cdots d\omega_{k-1}}{\pi^{k-1}}\tilde{f}_t(-\omega_1)\Big[\tilde{S}_z(\omega_1)-\tilde{S}_x(\omega_1)\Big]\,\tilde{f}_t(\omega_{12})\prod_{i=2}^{k-2}\tilde{f}_t(\omega_{i,i+1})\Big[\sin^2\overline{\chi}\tilde{S}_z(\omega_i)+\cos^2\overline{\chi}\tilde{S}_x(\omega_i)\Big]$$
$$\tilde{f}_t(\omega_{k-1})\left[\tilde{S}_z(\omega_{k-1})-\tilde{S}_x(\omega_{k-1})\right], \tag{I.7}$$

where $\omega_{ij}\equiv\omega_i-\omega_j$. We identify two types of terms in the above result: *linked* terms (first line) with k correlators and *semi-linked* terms (lines 2-3) with $k-1$ correlators in the kth cumulant. These two contributions correspond to the linked ($R_k(t)$) and semi-linked ($\tilde{R}_k$) diagrams given in the main text in Eqs. (10)-(11).

* gramon@scu.edu
† lcyw@ifpan.edu.pl

II. AXIS-ERROR CONTRIBUTIONS

Here we provide details on the calculation of the axis tilting, transient term, in Eq. (8) in the main text. We begin by rewriting the time-dependent noise-induced error in the rotation angle, Eq. (6) in the main text, using distinct time dependence for each of the error terms:

$$2\delta\phi(t)=\lim_{t_i\to t}\Bigg\{\cos\overline{\chi}\int_0^{t_\alpha}dt' f_{t_\alpha}(t')\xi_z(t')+\sin\overline{\chi}\int_0^{t_\beta}dt' f_{t_\beta}(t')\xi_x(t')+\frac{\cos\overline{\chi}}{2B_z}\Big[\sin^2\overline{\chi}\times \int_0^{t_\gamma}dt' f_{t_\gamma}(t')\xi_z^2(t')+\cos^2\overline{\chi}\int_0^{t_\delta}dt' f_{t_\delta}(t')\xi_x^2(t')-\sin 2\overline{\chi}\int_0^{t_\epsilon}dt' f_{t_\epsilon}(t')\xi_z(t')\xi_x(t')\Big]\Bigg\}, \tag{II.1}$$

such that Eq. (12) in the main text is replaced with

$$\langle e^{\pm 2i\delta\phi}\rangle=\lim_{t_i\to t}\left[c_z(t_\alpha)c_x(t_\beta)e^{-\sum_{k=1}(\pm 1)^k R_k(t_\gamma,t_\delta,t_\epsilon)}e^{-\sum_{k=3}(\pm 1)^k\tilde{R}_k(t_\alpha,t_\beta,t_\gamma,t_\delta,t_\epsilon)}\right], \tag{II.2}$$

and we singled out the semi-linked diagram in the second cumulant, given by Eqs. (13) in the main text, to facilitate comparison with Ref. [1]. The identification of the time dependencies of individual noise terms in the linked and semi-linked diagrams (calculated explicitly for low frequency noises in Section IV of the supplemental material) allows us to selectively differentiate with respect to the various t_i's and obtain the axis-tilting error contribution, as well as the corresponding contribution, W_T, given in Eq. (III.4) below, for the return probabilities in specific experimental scenarios. Recalling that $f_t(t)=(-1)^n$, where n is the number of control pulses, we find

$$\begin{aligned}
\langle\xi_z e^{\pm 2i\delta\phi}\rangle&=\frac{\mp i(-1)^n}{\cos\overline{\chi}}\lim_{t_i\to t}\left[\frac{\dot{c}_z(t_\alpha)}{c_z(t_\alpha)}-\sum_{k=3}(\pm 1)^k\frac{\partial\tilde{R}(t_\alpha,t_\beta,t_\gamma,t_\delta,t_\epsilon)}{\partial t_\alpha}\right]\langle e^{\pm 2i\delta\phi}\rangle\\
\langle\xi_x e^{\pm 2i\delta\phi}\rangle&=\frac{\mp i(-1)^n}{\sin\overline{\chi}}\lim_{t_i\to t}\left[\frac{\dot{c}_x(t_\beta)}{c_x(t_\beta)}-\sum_{k=3}(\pm 1)^k\frac{\partial\tilde{R}_k(t_\alpha,t_\beta,t_\gamma,t_\delta,t_\epsilon)}{\partial t_\beta}\right]\langle e^{\pm 2i\delta\phi}\rangle\\
\langle\xi_z^2 e^{\pm 2i\delta\phi}\rangle&=\frac{\pm 2i(-1)^n B_z}{\cos\overline{\chi}\sin^2\overline{\chi}}\lim_{t_i\to t}\left[\sum_{k=1}(\pm 1)^k\frac{\partial R_k(t_\gamma,t_\delta,t_\epsilon)}{\partial t_\gamma}+\sum_{k=3}(\pm 1)^k\frac{\partial\tilde{R}_k(t_\alpha,t_\beta,t_\gamma,t_\delta,t_\epsilon)}{\partial t_\gamma}\right]\langle e^{\pm 2i\delta\phi}\rangle\\
\langle\xi_x^2 e^{\pm 2i\delta\phi}\rangle&=\frac{\pm 2i(-1)^n B_z}{\cos^3\overline{\chi}}\lim_{t_i\to t}\left[\sum_{k=1}(\pm 1)^k\frac{\partial R_k(t_\gamma,t_\delta,t_\epsilon)}{\partial t_\delta}+\sum_{k=3}(\pm 1)^k\frac{\partial\tilde{R}_k(t_\alpha,t_\beta,t_\gamma,t_\delta,t_\epsilon)}{\partial t_\delta}\right]\langle e^{\pm 2i\delta\phi}\rangle\\
\langle\xi_z\xi_x e^{\pm 2i\delta\phi}\rangle&=\frac{\mp i(-1)^n B_z}{\cos^2\overline{\chi}\sin\overline{\chi}}\lim_{t_i\to t}\left[\sum_{k=1}(\pm 1)^k\frac{\partial R_k(t_\gamma,t_\delta,t_\epsilon)}{\partial t_\epsilon}+\sum_{k=3}(\pm 1)^k\frac{\partial\tilde{R}_k(t_\alpha,t_\beta,t_\gamma,t_\delta,t_\epsilon)}{\partial t_\epsilon}\right]\langle e^{\pm 2i\delta\phi}\rangle.
\end{aligned} \tag{II.3}$$

Denoting

$$\dot{\Sigma}_k^i\equiv\lim_{\substack{t_j\to t\\ j=\alpha,\beta,\gamma}}\sum_k\frac{\partial R_k(t_\gamma,t_\delta,t_\epsilon)}{\partial t_i},\qquad \dot{\tilde{\Sigma}}_k^i\equiv\lim_{\substack{t_j\to t\\ j=\alpha,\beta,\gamma,\delta,\epsilon}}\sum_k\frac{\partial\tilde{R}_k(t_\alpha,t_\beta,t_\gamma,t_\delta,t_\epsilon)}{\partial t_i}, \tag{II.4}$$

we find the axis tilting error term in Eq. (8) in the main text as

$$-\frac{1}{2}\left\langle\delta\chi^2\left[\cos 2\phi+e^{-2i\phi}\right]\right\rangle=\frac{(-1)^n}{B}c_z(t)c_x(t)e^{-(\Sigma_{2k}+\tilde{\Sigma}_{2k})}\Bigg\{\left[\left(\dot{\Sigma}_{2k}^\gamma+\dot{\Sigma}_{2k}^\delta+\dot{\Sigma}_{2k}^\epsilon\right)+\left(\dot{\tilde{\Sigma}}_{2k}^\gamma+\dot{\tilde{\Sigma}}_{2k}^\delta+\dot{\tilde{\Sigma}}_{2k}^\epsilon\right)\right]\times \left(\sin 2\tilde{\phi}+\frac{i}{2}e^{-2i\tilde{\phi}}\right)-\left[\left(\dot{\Sigma}_{2k+1}^\gamma+\dot{\Sigma}_{2k+1}^\delta+\dot{\Sigma}_{2k+1}^\epsilon\right)+\left(\dot{\tilde{\Sigma}}_{2k+1}^\gamma+\dot{\tilde{\Sigma}}_{2k+1}^\delta+\dot{\tilde{\Sigma}}_{2k+1}^\epsilon\right)\right]\left(\cos 2\tilde{\phi}+\frac{1}{2}e^{-2i\tilde{\phi}}\right)\Bigg\} \tag{II.5}$$

where

$$\tilde{\phi}=\overline{\phi}+\frac{1}{2}\left(\Sigma_{2k+1}+\tilde{\Sigma}_{2k+1}\right). \tag{II.6}$$

III. RETURN PROBABILITIES IN RECENT EXPERIMENTS

Here we calculate return probabilities for two, often-encountered experimental setups for singlet-triplet qubits: (i) preparing the qubit in a singlet state, letting it precess (freely or under DD pulse sequence) for time t at position $\delta h\gg J$ and measuring

singlet return probability, $P_S(t)$, as was done, e.g., in [2] to obtain the noise spectrum of the nuclear environment; (ii) preparing the qubit in a singlet state, adiabatically ramping detuning to bring the qubit to the $|\uparrow\downarrow\rangle$ (the ground state for $\delta h \gg J$ position), followed by a rapid increase in J to allow qubit evolution for time t at $J \gg \delta h$, and readout to measure return probability $P_{\uparrow\downarrow}(t)$ [3]. In both scenarios, the DQD potential is initially tilted to form a $(0,2)$ charge configuration, so that the qubit is initialized in a singlet state. Qubit precession is then measured either between S and T_0 (in (i)) or between $|\uparrow\downarrow\rangle$ and $|\downarrow\uparrow\rangle$ (in (ii)), exposing the qubit predominantly to nuclear or charge noise, respectively.

Using the expansions in Eqs. (5) and (6), we calculate return probabilities by performing Gaussian averaging over both ξ_z and ξ_x noises, as was done to obtain Eq. (8) in the main text. For the two scenarios above, we have, to second order in ξ_l

$$\langle P_S(t)\rangle = 1 - \langle \sin^2\chi(t)\sin^2\phi(t)\rangle = 1 - \frac{1}{2}\sin^2\overline{\chi}\left[1-\cos 2\overline{\phi}W_D(t)\left(1+\csc^2\overline{\chi}W_T(t)\right)\right] \tag{III.1}$$

and

$$\langle P_{\uparrow\downarrow}(t)\rangle = 1 - \langle \cos^2\chi(t)\sin^2\phi(t)\rangle = 1 - \frac{1}{2}\cos^2\overline{\chi}\left[1-\cos 2\overline{\phi}W_D(t)\left(1+\sec^2\overline{\chi}W_T(t)\right)\right], \tag{III.2}$$

where $\langle\cdot\rangle$ denotes averaging over both ξ_z and ξ_x. The dominant contribution to decoherence in these return probabilities, $W_D(t)$ is due to accumulated rotation angle errors, $\delta\phi$, and is found using Eq. (12) in the main text as

$$W_D(t) = \frac{\langle\cos 2\phi(t)\rangle}{\cos 2\overline{\phi}} = \langle\cos 2\delta\phi\rangle - \tan 2\overline{\phi}\,\langle\sin 2\delta\phi\rangle = \frac{\cos 2\tilde{\phi}}{\cos 2\overline{\phi}}c_z(t)c_x(t)e^{-\left[\Sigma_{2k}+\tilde{\Sigma}_{2k}\right]}, \tag{III.3}$$

where $c_z(t)$ and $c_x(t)$ were given in Eqs. (13) in the main text, and $\tilde{\phi}$ was defined in Eq. (II.6) above. The small transient contribution due to axis tilting errors is captured by $W_T(t)$, which we find as

$$\begin{aligned} W_T(t) = {} & \frac{\sin^2 2\overline{\chi}}{2W_D(t)\cos 2\overline{\phi}}\left\langle\cos 2\phi(t)\left(\frac{\xi_x}{B_x}-\frac{\xi_z}{B_z}\right)\left[1-\frac{1}{2}\left(\frac{\xi_x}{B_x}+\frac{\xi_z}{B_z}\right)+\cos 2\overline{\chi}\left(\frac{\xi_x}{B_x}-\frac{\xi_z}{B_z}\right)\right]\right\rangle = \\ & \frac{2(-1)^n}{B}\left\{\left[\cos^2\overline{\chi}\left(\frac{\dot{c}_x(t)}{c_x(t)}-\dot{\tilde{\Sigma}}^{\beta}_{2k}\right)-\sin^2\overline{\chi}\left(\frac{\dot{c}_z(t)}{c_z(t)}-\dot{\tilde{\Sigma}}^{\alpha}_{2k}\right)-(2\cos 2\overline{\chi}+1)\left(\dot{\Sigma}^{\gamma}_{2k}+\dot{\tilde{\Sigma}}^{\gamma}_{2k}\right)-\right.\right. \\ & (2\cos 2\overline{\chi}-1)\left(\dot{\Sigma}^{\delta}_{2k}+\dot{\tilde{\Sigma}}^{\delta}_{2k}\right)-2\cos 2\overline{\chi}\left(\dot{\Sigma}^{\epsilon}_{2k}+\dot{\tilde{\Sigma}}^{\epsilon}_{2k}\right)\Big]\tan 2\tilde{\phi}+\Big[\cos^2\overline{\chi}\dot{\tilde{\Sigma}}^{\beta}_{2k+1}-\sin^2\overline{\chi}\dot{\tilde{\Sigma}}^{\alpha}_{2k+1}+ \\ & \left.\left.(2\cos 2\overline{\chi}+1)\left(\dot{\Sigma}^{\gamma}_{2k+1}+\dot{\tilde{\Sigma}}^{\gamma}_{2k+1}\right)+(2\cos 2\overline{\chi}-1)\left(\dot{\Sigma}^{\delta}_{2k+1}+\dot{\tilde{\Sigma}}^{\delta}_{2k+1}\right)+2\cos 2\overline{\chi}\left(\dot{\Sigma}^{\epsilon}_{2k+1}+\dot{\tilde{\Sigma}}^{\epsilon}_{2k+1}\right)\Big]\right\}. \end{aligned} \tag{III.4}$$

IV. DETAILS OF CUMULANT RESUMMATION FOR LOW-FREQUENCY NOISES

The evaluation of the linked and semi-linked diagrams in Eqs. (10)-(11) in the main text, and their time derivatives in Eqs. (II.3) above, is made possible by reexpressing them in terms of time integrals:

$$\begin{aligned} R_k(t_\gamma,t_\delta,t_\epsilon) = {} & -\frac{1}{2}\left(\frac{i}{B}\right)^k\sum_{m=0}^{\lfloor\frac{k}{2}\rfloor}\frac{\sin^{2m}2\overline{\chi}}{2^{3m}(k-m)}\binom{k-m}{m}\int dt_1\cdots dt_k\prod_{\substack{i=1\\(k+1\to 1)}}^{k-2m}\left[\sin^2\overline{\chi}f_{t_\gamma}(t_i)S_z(t_{i,i+1})+\cos^2\overline{\chi}f_{t_\delta}(t_i)S_x(t_{i,i+1})\right]\times \\ & \prod_{\substack{j=k-2m+1:2:k\\(k+1\to 1)}}\left[f_{t_\epsilon}(t_j)f_{t_\epsilon}(t_{j+1})-f_{t_\gamma}(t_j)f_{t_\delta}(t_{j+1})\right]\left[S_z(t_{j,j+1})S_x(t_{j+1,j+2})+S_x(t_{j,j+1})S_z(t_{j+1,j+2})\right], \end{aligned} \tag{IV.1}$$

and

$$\tilde{R}_k(t_\alpha,t_\beta,t_\gamma,t_\delta,t_\epsilon)=-\frac{1}{2}\left(\frac{i}{B}\right)^k(B_z\sin\overline{\chi})^2\int dt_1\cdots dt_k\left\{\left[f_{t_\alpha}(t_1)f_{t_\alpha}(t_2)f_{t_\gamma}(t_k)S_z(t_{12})S_z(t_{k-1,k})+\right.\right.$$
$$\left.f_{t_\beta}(t_1)f_{t_\beta}(t_2)f_{t_\delta}(t_k)S_h(t_{12})S_x(t_{k-1,k})-f_{t_\alpha}(t_1)f_{t_\beta}(t_2)f_{t_\epsilon}(t_k)\left(S_z(t_{12})S_x(t_{k-1,k})+S_x(t_{12})S_z(t_{k-1,k})\right)\right]$$
$$\sum_{m=0}^{\lfloor\frac{k-3}{2}\rfloor}\frac{\sin^{2m}2\overline{\chi}}{2^{3m}}\binom{k-m-3}{m}\prod_{i=2}^{k-2(m+1)}\left[\sin^2\overline{\chi}f_{t_\gamma}(t_{i+1})S_z(t_{i,i+1})+\cos^2\overline{\chi}f_{t_\delta}(t_{i+1})S_x(t_{i,i+1})\right]\times$$
$$\prod_{j=k-2m-1:2:k-3}\left[f_{t_\epsilon}(t_{j+1})f_{t_\epsilon}(t_{j+2})-f_{t_\gamma}(t_{j+1})f_{t_\delta}(t_{j+2})\right]\left[S_z(t_{j,j+1})S_x(t_{j+1,j+2})+S_x(t_{j,j+1})S_z(t_{j+1,j+2})\right]+$$
$$\frac{1}{2}\left[\cos^2\overline{\chi}f_{t_\alpha}(t_1)f_{t_\alpha}(t_2)S_z(t_{12})+\sin^2\overline{\chi}f_{t_\beta}(t_1)f_{t_\beta}(t_2)S_x(t_{12})\right]\sum_{m=0}^{\lfloor\frac{k-4}{2}\rfloor}\frac{\sin^{2m}2\overline{\chi}}{2^{3m}}\binom{k-m-4}{m}\times$$
$$\prod_{i=2}^{k-2m-3}\left[\sin^2\overline{\chi}f_{t_\gamma}(t_{i+1})S_z(t_{i,i+1})+\cos^2\overline{\chi}f_{t_\delta}(t_{i+1})S_x(t_{i,i+1})\right]\prod_{j=k-2m-2:2:k-2}\left[f_{t_\epsilon}(t_{j+1})f_{t_\epsilon}(t_{j+2})-f_{t_\gamma}(t_{j+1})f_{t_\delta}(t_{j+2})\right]\times$$
$$\left.\left[S_z(t_{j,j+1})S_x(t_{j+1,j+2})+S_x(t_{j,j+1})S_z(t_{j+1,j+2})\right]\right\}. \tag{IV.2}$$

In the above expressions, we have kept explicit time dependencies, t_i, corresponding to the various noise terms, to facilitate the evaluation of the transient axis-tilting error contributions (see Section II of the supplemental material). It can be verified directly that in the limit $t_i\to t$, Eqs. (IV.1)-(IV.2) reduce to Eqs. (10)-(11) in the main text.

In what follows, we assume a DD scenario and discuss the FID case separately below. Replacing each noise correlator in Eqs. (IV.1)-(IV.2) with $S_l(t_{ij})=\langle\xi_l^{\rm hf}(t_i)\xi_l^{\rm hf}(t_j)\rangle_{\rm hf}+\sigma_{0l}^2$, and keeping only terms with maximal power of σ_{0l}^2, the even and odd linked diagrams read

$$R_{2k}(t_\gamma,t_\delta,t_\epsilon)=\frac{(-1)^{k+1}}{B^{2k}}\sum_{m=0}^{k}\frac{1}{2k-m}\binom{2k-m}{m}\left[s\sigma_1(t_\gamma,t_\delta)\right]^{k-m}\left[s\sigma_2(t_\gamma,t_\delta,t_\epsilon)\right]^m, \tag{IV.3}$$

$$R_{2k+1}(t_\gamma,t_\delta,t_\epsilon)=\frac{i(-1)^{k+1}}{2B^{2k+1}}\left[\sin^2\overline{\chi}\sigma_{0z}^2\tilde{f}_{t_\gamma}(0)+\cos^2\overline{\chi}\sigma_{0x}^2\tilde{f}_{t_\delta}(0)\right]\sum_{m=0}^{k}\frac{1}{2k+1-m}\binom{2k+1-m}{m}\left[s\sigma_1(t_\gamma,t_\delta)\right]^{k-m}\times$$
$$\left[s\sigma_2(t_\gamma,t_\delta,t_\epsilon)\right]^m, \tag{IV.4}$$

where we defined

$$s\sigma_1(t_\gamma,t_\delta)=\int_0^\infty\frac{d\omega}{\pi}\left[\sin^4\overline{\chi}\left|\tilde{f}_{t_\gamma}(\omega)\right|^2\tilde{S}_z^{\rm hf}(\omega)\sigma_{0z}^2+\cos^4\overline{\chi}\left|\tilde{f}_{t_\delta}(\omega)\right|^2\tilde{S}_x^{\rm hf}(\omega)\sigma_{0x}^2+\right.$$
$$\left.\frac{1}{8}\sin^2 2\overline{\chi}\left(\tilde{f}_{t_\gamma}(\omega)\tilde{f}_{t_\delta}^*(\omega)+h.c.\right)\left(\tilde{S}_z^{\rm hf}(\omega)\sigma_{0x}^2+\tilde{S}_x^{\rm hf}(\omega)\sigma_{0z}^2\right)\right] \tag{IV.5}$$

and

$$s\sigma_2(t_\gamma,t_\delta,t_\epsilon)=\frac{\sin^2 2\overline{\chi}}{8}\int_0^\infty\frac{d\omega}{\pi}\left[\left|\tilde{f}_{t_\epsilon}(\omega)\right|^2-\frac{1}{2}\left(\tilde{f}_{t_\gamma}(\omega)\tilde{f}_{t_\delta}^*(\omega)+h.c.\right)\right]\left(\tilde{S}_z^{\rm hf}(\omega)\sigma_{0x}^2+\tilde{S}_x^{\rm hf}(\omega)\sigma_{0z}^2\right), \tag{IV.6}$$

and denoted $\tilde{S}_l^{\rm hf}(\omega)$ as the high-frequency part of the noise spectra (see main text below Eq. (17)). The even and odd semi-linked diagrams read

$$\tilde{R}_{2k}(t_\alpha,t_\beta,t_\gamma,t_\delta,t_\epsilon)=\frac{(-1)^{k+1}}{2B^{2k}}\left\{\left(\frac{B_xB_z}{B}\right)^2\left(F_1^{(2k)}+G_1^{(2k)}\right)\sum_{m=0}^{k-2}\binom{2k-m-3}{m}\left[s\sigma_1(t_\gamma,t_\delta)\right]^{k-m-2}\left[s\sigma_2(t_\gamma,t_\delta,t_\epsilon)\right]^m+\right.$$
$$\left.B^2\left(F_2^{(2k)}+G_2^{(2k)}\right)\sum_{m=0}^{k-2}\binom{2k-m-4}{m}\left[s\sigma_1(t_\gamma,t_\delta)\right]^{k-m-2}\left[s\sigma_2(t_\gamma,t_\delta,t_\epsilon)\right]^{m+1}\right\}, \tag{IV.7}$$

and

$$\tilde{R}_{2k+1}(t_\alpha,t_\beta,t_\gamma,t_\delta,t_\epsilon)=\frac{i(-1)^{k+1}}{2B^{2k+1}}\left\{\left(\frac{B_xB_z}{B}\right)^2F_1^{(2k+1)}\sum_{m=0}^{k-1}\binom{2k-m-2}{m}\left[s\sigma_1(t_\gamma,t_\delta)\right]^{k-m-1}\left[s\sigma_2(t_\gamma,t_\delta,t_\epsilon)\right]^m+\right.$$
$$\left.B^2F_2^{(2k+1)}\sum_{m=0}^{k-2}\binom{2k-m-3}{m}\left[s\sigma_1(t_\gamma,t_\delta)\right]^{k-m-2}\left[s\sigma_2(t_\gamma,t_\delta,t_\epsilon)\right]^{m+1}\right\}. \tag{IV.8}$$

In the above equations:

$$F_1^{(2k)} = \sigma_{0z}^4 \tilde{f}_{t_\alpha}^2(0)\left[\sin^2\overline{\chi} S_z^{\rm hf}(t_\gamma,t_\gamma)+\cos^2\overline{\chi} S_x^{\rm hf}(t_\gamma,t_\delta)\right]+\sigma_{0x}^4 \tilde{f}_{t_\beta}^2(0)\left[\sin^2\overline{\chi} S_z^{\rm hf}(t_\delta,t_\gamma)+\cos^2\overline{\chi} S_x^{\rm hf}(t_\delta,t_\delta)\right] - 2\sigma_{0z}^2\sigma_{0x}^2\tilde{f}_{t_\alpha}(0)\tilde{f}_{t_\beta}(0)\left[\sin^2\overline{\chi} S_z^{\rm hf}(t_\epsilon,t_\gamma)+\cos^2\overline{\chi} S_x^{\rm hf}(t_\epsilon,t_\delta)\right]$$
$$F_2^{(2k)} = \sigma_{0z}^2\tilde{f}_{t_\alpha}^2(0)\cos^2\overline{\chi}+\sigma_{0x}^2\tilde{f}_{t_\beta}^2(0)\sin^2\overline{\chi}, \tag{IV.9}$$

$$G_1^{(2k)} = \sigma_{0z}^2\sin^2\overline{\chi}\left[S_z^{\rm hf}(t_\alpha,t_\gamma)S_z^{\rm hf}(t_\gamma,t_\alpha)+S_x^{\rm hf}(t_\beta,t_\delta)S_x^{\rm hf}(t_\gamma,t_\beta)-S_z^{\rm hf}(t_\alpha,t_\epsilon)S_x^{\rm hf}(t_\gamma,t_\beta)-S_x^{\rm hf}(t_\alpha,t_\epsilon)S_z^{\rm hf}(t_\gamma,t_\beta)\right]+ \sigma_{0x}^2\cos^2\overline{\chi}\left[S_z^{\rm hf}(t_\alpha,t_\gamma)S_z^{\rm hf}(t_\delta,t_\alpha)+S_x^{\rm hf}(t_\beta,t_\delta)S_x^{\rm hf}(t_\delta,t_\beta)-S_z^{\rm hf}(t_\alpha,t_\epsilon)S_x^{\rm hf}(t_\delta,t_\beta)-S_x^{\rm hf}(t_\alpha,t_\epsilon)S_z^{\rm hf}(t_\delta,t_\beta)\right]$$
$$G_2^{(2k)} = \cos^2\overline{\chi}S_z^{\rm hf}(t_\alpha,t_\alpha)+\sin^2\overline{\chi}S_x^{\rm hf}(t_\beta,t_\beta) \tag{IV.10}$$

and

$$F_1^{(2k+1)} = \sigma_{0z}^2\left[\tilde{f}_{t_\gamma}(0)S_z^{\rm hf}(t_\alpha,t_\alpha)+\tilde{f}_{t_\alpha}(0)S_z^{\rm hf}(t_\alpha,t_\gamma)-\tilde{f}_{t_\alpha}(0)S_x^{\rm hf}(t_\beta,t_\epsilon)-\tilde{f}_{t_\epsilon}(0)S_x^{\rm hf}(t_\alpha,t_\beta)\right]+ \sigma_{0x}^2\left[\tilde{f}_{t_\delta}(0)S_x^{\rm hf}(t_\beta,t_\beta)+\tilde{f}_{t_\beta}(0)S_x^{\rm hf}(t_\beta,t_\delta)-\tilde{f}_{t_\beta}(0)S_z^{\rm hf}(t_\alpha,t_\epsilon)-\tilde{f}_{t_\epsilon}(0)S_z^{\rm hf}(t_\alpha,t_\beta)\right]$$
$$F_2^{(2k+1)} = \tilde{f}_{t_\alpha}(0)\sigma_{0z}^2\cos^2\overline{\chi}\left[\sin^2\overline{\chi}S_z^{\rm hf}(t_\alpha,t_\gamma)+\cos^2\overline{\chi}S_x^{\rm hf}(t_\alpha,t_\delta)\right]+\tilde{f}_{t_\beta}(0)\sigma_{0x}^2\sin^2\overline{\chi}\left[\sin^2\overline{\chi}S_z^{\rm hf}(t_\beta,t_\gamma)+ \cos^2\overline{\chi}S_x^{\rm hf}(t_\beta,t_\delta)\right]+\left[\sin^2\overline{\chi}\tilde{f}_{t_\gamma}(0)\sigma_{0z}^2+\cos^2\overline{\chi}\tilde{f}_{t_\delta}(0)\sigma_{0x}^2\right]\left[\sin^2\overline{\chi}S_x^{\rm hf}(t_\beta,t_\beta)+\cos^2\overline{\chi}S_z^{\rm hf}(t_\alpha,t_\alpha)\right], \tag{IV.11}$$

where we have defined

$$S_l^{\rm hf}(t_i,t_j) \equiv \int_0^\infty \frac{d\omega}{2\pi}\left[\tilde{f}_{t_i}(\omega)\tilde{f}_{t_j}^*(\omega)+h.c.\right]\tilde{S}_l^{\rm hf}(\omega), \tag{IV.12}$$

such that

$$S_l^{\rm hf}(t_i,t_j)\big|_{t_i,t_j\to t} \equiv S_l^{\rm hf}(t) = \int_{\omega_1}^\infty \frac{d\omega}{\pi}\left|\tilde{f}_t(\omega)\right|^2\tilde{S}_l(\omega). \tag{IV.13}$$

Within the low-frequency noise approximation, the above formulae for the linked and semi-linked terms can be shown to converge to their original expressions, Eqs. (10)-(11) in the main text, when the $t_i \to t$ limit is taken. Notice that $\tilde{f}_t(0) = \int f_t(t')dt' = t$ for the case of FID, otherwise for any balanced pulse sequence it is zero. As a result, under any DD pulse sequence, all odd terms and their derivatives vanish to leading order. We provide their expressions and summations here for completeness and to facilitate the FID results stated at the end of this section. Sub-leading terms to $R_{2k+1}(t)$ and its derivatives that are nonzero for balanced sequences, are provided in Section V of the supplemental material, but their contribution is negligible for any experimentally-relevant noise parameters. Similarly, the semi-linked even terms, $\tilde{R}_{2k}(t)$, given in Eq. (IV.7) include $A_i^{(2k)}$ (leading) contributions that vanish except for FID and $B_i^{(2k)}$ (sub-leading) contributions with one less σ_{0l}^2 factor, that remain nonzero in all cases [see Eqs. (IV.9)-(IV.10)].

We can now carry out the explicit time derivatives needed to evaluate the axis-tilting contributions in Eqs. (II.5) and (III.4). Using $S_\pm^{\rm hf}(t)$, $\overline{S}_\pm^{\rm hf}(t)$, and $\sigma_{0\pm}^2$, $\overline{\sigma}_{0\pm}^2$, defined below Eq. (**??**) in the main text, we find

$$\left.\frac{\partial R_{2k}}{\partial t_\gamma}\right|_{t_i\to t} = \frac{(-1)^{k+1}}{2B^{2k}}\left[\overline{\sigma}_{0+}^2\overline{S}_+^{\rm hf}(t)\right]^{k-1}\sin^4\overline{\chi}\sigma_{0z}^2\dot{S}_z^{\rm hf}(t)$$
$$\left.\frac{\partial R_{2k}}{\partial t_\delta}\right|_{t_i\to t} = \frac{(-1)^{k+1}}{2B^{2k}}\left[\overline{\sigma}_{0+}^2\overline{S}_+^{\rm hf}(t)\right]^{k-1}\cos^4\overline{\chi}\sigma_{0x}^2\dot{S}_x^{\rm hf}(t)$$
$$\left.\frac{\partial R_{2k}}{\partial t_\epsilon}\right|_{t_i\to t} = \frac{(-1)^{k}}{8B^{2k}}\left[\overline{\sigma}_{0+}^2\overline{S}_+^{\rm hf}(t)\right]^{k-1}\sin^2 2\overline{\chi}\left[\sigma_{0x}^2\dot{S}_z^{\rm hf}(t)+\sigma_{0z}^2\dot{S}_x^{\rm hf}(t)\right], \tag{IV.14}$$

$$i\left.\frac{\partial R_{2k+1}}{\partial t_\gamma}\right|_{t_i\to t} = \frac{(-1)^{k}}{2B^{2k+1}}\left[\overline{\sigma}_{0+}^2\overline{S}_+^{\rm hf}(t)\right]^{k}\left[\frac{\tilde{f}_t(0)}{\overline{S}_+^{\rm hf}(t)}\left(\frac{k}{2k+1}\frac{\partial s\sigma_1}{\partial t_\gamma}+\frac{\partial s\sigma_2}{\partial t_\gamma}\right)+\frac{\sin^2\overline{\chi}}{2k+1}\dot{\tilde{f}}_t(0)\sigma_{0z}^2\right]$$
$$i\left.\frac{\partial R_{2k+1}}{\partial t_\delta}\right|_{t_i\to t} = \frac{(-1)^{k}}{2B^{2k+1}}\left[\overline{\sigma}_{0+}^2\overline{S}_+^{\rm hf}(t)\right]^{k}\left[\frac{\tilde{f}_t(0)}{\overline{S}_+^{\rm hf}(t)}\left(\frac{k}{2k+1}\frac{\partial s\sigma_1}{\partial t_\delta}+\frac{\partial s\sigma_2}{\partial t_\delta}\right)+\frac{\cos^2\overline{\chi}}{2k+1}\dot{\tilde{f}}_t(0)\sigma_{0x}^2\right]$$
$$i\left.\frac{\partial R_{2k+1}}{\partial t_\epsilon}\right|_{t_i\to t} = \frac{(-1)^{k}}{2B^{2k+1}}\left[\overline{\sigma}_{0+}^2\overline{S}_+^{\rm hf}(t)\right]^{k}\frac{\tilde{f}_t(0)}{\overline{S}_+^{\rm hf}(t)}\frac{\partial s\sigma_2}{\partial t_\epsilon} \tag{IV.15}$$

and

$$\left.\frac{\partial\tilde{R}_{2k}}{\partial t_\alpha}\right|_{t_i\to t}=\frac{(-1)^{k+1}(B_xB_z)^2}{2B^{2k+2}}\left[\overline{\sigma}_{0+}^2\overline{S}_+^{\rm hf}(t)\right]^{k-2}\left[2\tilde{f}_t(0)\dot{\tilde{f}}_t(0)\sigma_{0z}^2\sigma_{0-}^2\overline{S}_+^{\rm hf}(t)+\frac{1}{2}\overline{\sigma}_{0+}^2\frac{d}{dt}\left(S_z^{\rm hf}(t)S_-^{\rm hf}(t)\right)\right]$$

$$\left.\frac{\partial\tilde{R}_{2k}}{\partial t_\beta}\right|_{t_i\to t}=\frac{(-1)^{k}(B_xB_z)^2}{2B^{2k+2}}\left[\overline{\sigma}_{0+}^2\overline{S}_+^{\rm hf}(t)\right]^{k-2}\left[2\tilde{f}_t(0)\dot{\tilde{f}}_t(0)\sigma_{0x}^2\sigma_{0-}^2\overline{S}_+^{\rm hf}(t)+\frac{1}{2}\overline{\sigma}_{0+}^2\frac{d}{dt}\left(S_x^{\rm hf}(t)S_-^{\rm hf}(t)\right)\right]$$

$$\left.\frac{\partial\tilde{R}_{2k}}{\partial t_\gamma}\right|_{t_i\to t}=\frac{(-1)^{k+1}(B_xB_z)^2}{2B^{2k+2}}\left[\overline{\sigma}_{0+}^2\overline{S}_+^{\rm hf}(t)\right]^{k-2}\left\{\frac{\tilde{f}_t^2(0)}{2}\left[\sigma_{0-}^4\dot{S}_z^{\rm hf}(t)\sin^2\overline{\chi}+\sigma_{0z}^4\dot{\overline{S}}_+^{\rm hf}(t)\right]+\frac{1}{2}\left[\overline{\sigma}_{0+}^2\dot{S}_z^{\rm hf}(t)S_z^{\rm hf}(t)+\right.\right.$$
$$\left.\left.\sigma_{0z}^2\dot{S}_-^{\rm hf}(t)S_-^{\rm hf}(t)\sin^2\overline{\chi}\right]+(k-2)\left[\frac{\tilde{f}_t^2(0)\sigma_{0-}^4}{\overline{\sigma}_{0+}^2}+\frac{\left[S_-^{\rm hf}(t)\right]^2}{\overline{S}_+^{\rm hf}(t)}\right]\left(\frac{\partial s\sigma_1}{\partial t_\gamma}+2\frac{\partial s\sigma_2}{\partial t_\gamma}\right)+\left(\frac{B^2}{B_xB_z}\right)^2\left[\tilde{f}_t^2(0)\overline{\sigma}_{0+}^2+\overline{S}_+^{\rm hf}(t)\right]\frac{\partial s\sigma_2}{\partial t_\gamma}\right\},$$

$$\left.\frac{\partial\tilde{R}_{2k}}{\partial t_\delta}\right|_{t_i\to t}=\frac{(-1)^{k+1}(B_xB_z)^2}{2B^{2k+2}}\left[\overline{\sigma}_{0+}^2\overline{S}_+^{\rm hf}(t)\right]^{k-2}\left\{\frac{\tilde{f}_t^2(0)}{2}\left[\sigma_{0-}^4\dot{S}_x^{\rm hf}(t)\cos^2\overline{\chi}+\sigma_{0x}^4\dot{\overline{S}}_+^{\rm hf}(t)\right]+\frac{1}{2}\left[\overline{\sigma}_{0+}^2\dot{S}_x^{\rm hf}(t)S_x^{\rm hf}(t)+\right.\right.$$
$$\left.\left.\sigma_{0x}^2\dot{S}_-^{\rm hf}(t)S_-^{\rm hf}(t)\cos^2\overline{\chi}\right]+(k-2)\left[\frac{\tilde{f}_t^2(0)\sigma_{0-}^4}{\overline{\sigma}_{0+}^2}+\frac{\left[S_-^{\rm hf}(t)\right]^2}{\overline{S}_+^{\rm hf}(t)}\right]\left(\frac{\partial s\sigma_1}{\partial t_\delta}+2\frac{\partial s\sigma_2}{\partial t_\delta}\right)+\left(\frac{B^2}{B_xB_z}\right)^2\left[\tilde{f}_t^2(0)\overline{\sigma}_{0+}^2+\overline{S}_+^{\rm hf}(t)\right]\frac{\partial s\sigma_2}{\partial t_\delta}\right\},$$

$$\left.\frac{\partial\tilde{R}_{2k}}{\partial t_\epsilon}\right|_{t_i\to t}=\frac{(-1)^{k+1}(B_xB_z)^2}{2B^{2k+2}}\left[\overline{\sigma}_{0+}^2\overline{S}_+^{\rm hf}(t)\right]^{k-2}\left\{-\tilde{f}_t^2(0)\sigma_{0z}^2\sigma_{0x}^2\dot{\overline{S}}_+^{\rm hf}(t)-\frac{1}{2}\overline{\sigma}_{0+}^2\frac{d}{dt}\left(S_z^{\rm hf}(t)S_x^{\rm hf}(t)\right)+\right.$$
$$\left.\left[2(k-2)\left(\frac{\tilde{f}_t^2(0)\sigma_{0-}^4}{\overline{\sigma}_{0+}^2}+\frac{\left[S_-^{\rm hf}(t)\right]^2}{\overline{S}_+^{\rm hf}(t)}\right)+\left(\frac{B^2}{B_xB_z}\right)^2\left(\tilde{f}_t^2(0)\overline{\sigma}_{0+}^2+\overline{S}_+^{\rm hf}(t)\right)\right]\frac{\partial s\sigma_2}{\partial t_\delta}\right\},\tag{IV.16}$$

$$i\left.\frac{\partial\tilde{R}_{2k+1}}{\partial t_\alpha}\right|_{t_i\to t}=\frac{(-1)^{k}(B_xB_z)^2}{2B^{2k+3}}\left[\overline{\sigma}_{0+}^2\overline{S}_+^{\rm hf}(t)\right]^{k-1}\left\{\tilde{f}_t(0)\left[\frac{1}{2}\sigma_{0z}^2\dot{S}_-^{\rm hf}(t)+\sigma_{0-}^2\dot{S}_z^{\rm hf}(t)\right]+\dot{\tilde{f}}_t(0)\sigma_{0z}^2S_-^{\rm hf}(t)\right\}$$

$$i\left.\frac{\partial\tilde{R}_{2k+1}}{\partial t_\beta}\right|_{t_i\to t}=\frac{(-1)^{k+1}(B_xB_z)^2}{2B^{2k+3}}\left[\overline{\sigma}_{0+}^2\overline{S}_+^{\rm hf}(t)\right]^{k-1}\left\{\tilde{f}_t(0)\left[\frac{1}{2}\sigma_{0x}^2\dot{S}_-^{\rm hf}(t)+\sigma_{0-}^2\dot{S}_x^{\rm hf}(t)\right]+\dot{\tilde{f}}_t(0)\sigma_{0x}^2S_-^{\rm hf}(t)\right\}$$

$$i\left.\frac{\partial\tilde{R}_{2k+1}}{\partial t_\gamma}\right|_{t_i\to t}=\frac{(-1)^{k}(B_xB_z)^2}{2B^{2k+3}}\left[\overline{\sigma}_{0+}^2\overline{S}_+^{\rm hf}(t)\right]^{k-1}\left\{\sigma_{0z}^2\left[\frac{\tilde{f}_t(0)}{2}\dot{S}_z^{\rm hf}(t)+\dot{\tilde{f}}_t(0)S_z^{\rm hf}(t)\right]+2\tilde{f}_t(0)\frac{\sigma_{0-}^2S_-^{\rm hf}(t)}{\overline{\sigma}_{0+}^2\overline{S}_+^{\rm hf}(t)}\times\right.$$
$$\left.\left[(k-1)\frac{\partial s\sigma_1}{\partial t_\gamma}+2\left(k-1+\frac{\sigma_{0z}^2S_x^{\rm hf}(t)+\sigma_{0x}^2S_z^{\rm hf}(t)}{\sin^2 2\overline{\chi}\sigma_{0-}^2S_-^{\rm hf}(t)}\right)\frac{\partial s\sigma_2}{\partial t_\gamma}\right]\right\}$$

$$i\left.\frac{\partial\tilde{R}_{2k+1}}{\partial t_\delta}\right|_{t_i\to t}=\frac{(-1)^{k}(B_xB_z)^2}{2B^{2k+3}}\left[\overline{\sigma}_{0+}^2\overline{S}_+^{\rm hf}(t)\right]^{k-1}\left\{\sigma_{0h}^2\left[\frac{\tilde{f}_t(0)}{2}\dot{S}_x^{\rm hf}(t)+\dot{\tilde{f}}_t(0)S_x^{\rm hf}(t)\right]+2\tilde{f}_t(0)\frac{\sigma_{0-}^2S_-^{\rm hf}(t)}{\overline{\sigma}_{0+}^2\overline{S}_+^{\rm hf}(t)}\times\right.$$
$$\left.\left[(k-1)\frac{\partial s\sigma_1}{\partial t_\delta}+2\left(k-1+\frac{\sigma_{0z}^2S_x^{\rm hf}(t)+\sigma_{0x}^2S_J^{\rm hf}(t)}{\sin^2 2\overline{\chi}\sigma_{0-}^2S_-^{\rm hf}(t)}\right)\frac{\partial s\sigma_2}{\partial t_\delta}\right]\right\}$$

$$i\left.\frac{\partial\tilde{R}_{2k+1}}{\partial t_\epsilon}\right|_{t_i\to t}=\frac{(-1)^{k}(B_xB_z)^2}{2B^{2k+3}}\left[\overline{\sigma}_{0+}^2\overline{S}_+^{\rm hf}(t)\right]^{k-1}\left\{-\frac{\tilde{f}_t(0)}{2}\left(\dot{S}_x^{\rm hf}(t)\sigma_{0z}^2+\dot{S}_z^{\rm hf}(t)\sigma_{0x}^2\right)-\dot{\tilde{f}}_t(0)\left(S_z^{\rm hf}(t)\sigma_{0x}^2+S_x^{\rm hf}(t)\sigma_{0z}^2\right)+\right.$$
$$\left.4\tilde{f}_t(0)\frac{\sigma_{0-}^2S_-^{\rm hf}(t)}{\overline{\sigma}_{0+}^2\overline{S}_+^{\rm hf}(t)}\left[k-1+\frac{\sigma_{0z}^2S_h^{\rm hf}(t)+\sigma_{0x}^2S_J^{\rm hf}(t)}{\sin^2 2\overline{\chi}\sigma_{0-}^2S_-^{\rm hf}(t)}\right]\frac{\partial s\sigma_2}{\partial t_\epsilon}\right\}.\tag{IV.17}$$

In Eqs. (IV.14)-(IV.17) we used:

$$\begin{aligned}
\left.\frac{\partial s\sigma_1}{\partial t_\gamma}\right|_{t_i\to t} &= \frac{1}{2}\sin^2\overline{\chi}\left(\dot{S}_z^{\rm hf}(t)\overline{\sigma}_{0+}^2+\dot{\overline{S}}_+^{\rm hf}(t)\sigma_{0z}^2\right)\\
\left.\frac{\partial s\sigma_1}{\partial t_\delta}\right|_{t_i\to t} &= \frac{1}{2}\cos^2\overline{\chi}\left(\dot{S}_x^{\rm hf}(t)\overline{\sigma}_{0+}^2+\dot{\overline{S}}_+^{\rm hf}(t)\sigma_{0x}^2\right)\\
\left.\frac{\partial s\sigma_2}{\partial t_\epsilon}\right|_{t_i\to t} &= -2\left.\frac{\partial s\sigma_2}{\partial t_\gamma}\right|_{t_i\to t} = -2\left.\frac{\partial s\sigma_2}{\partial t_\delta}\right|_{t_i\to t} = \dot{S}_z^{\rm hf}(t)\sigma_{0x}^2+\dot{S}_x^{\rm hf}(t)\sigma_{0z}^2.
\end{aligned}\tag{IV.18}$$

Using Eqs. (IV.3)-(IV.11), we can carry out the cumulant summations resulting in Eqs. (15), (16) and (18) in the main text. Similarly, we use Eqs. (IV.14)-(IV.17) to derive explicit expressions for the various time derivatives of the cumulant sums as they appear in Eqs. (II.5) and (III.4). For odd sums (linked terms start at $k=0$, semi-linked terms start at $k=1$) we find:

$$\begin{aligned}
\left(\dot{\Sigma}_{2k+1}^{\gamma}+\dot{\Sigma}_{2k+1}^{\delta}+\dot{\Sigma}_{2k+1}^{\epsilon}\right) &= \frac{\overline{\sigma}_{0+}^2}{2}\left\{\frac{\tilde{f}_t(0)\dot{\overline{S}}_+^{\rm hf}(t)\eta(t)}{2B\overline{S}_+^{\rm hf}(t)}+\frac{\arctan\left(\frac{1}{B}\sqrt{\overline{\sigma}_{0+}^2\overline{S}_+^{\rm hf}(t)}\right)}{\sqrt{\overline{\sigma}_{0+}^2\overline{S}_+^{\rm hf}(t)}}\left(\dot{\tilde{f}}_t(0)-\frac{\tilde{f}_t(0)\dot{\overline{S}}_+^{\rm hf}(t)}{2\overline{S}_+^{\rm hf}(t)}\right)\right\}\\
\left(\dot{\Sigma}_{2k+1}^{\gamma}-\dot{\Sigma}_{2k+1}^{\delta}\right) &= \frac{\overline{\sigma}_{0-}^2}{2}\left\{\frac{\arctan\left(\frac{1}{B}\sqrt{\overline{\sigma}_{0+}^2\overline{S}_+^{\rm hf}(t)}\right)}{\sqrt{\overline{\sigma}_{0+}^2\overline{S}_+^{\rm hf}(t)}}\left[\dot{\tilde{f}}_t(0)-\frac{\tilde{f}_t(0)}{4\overline{S}_+^{\rm hf}(t)}\left(\dot{\overline{S}}_+^{\rm hf}(t)+\frac{\overline{\sigma}_{0+}^2}{\overline{\sigma}_{0-}^2}\dot{\overline{S}}_-^{\rm hf}(t)\right)\right]+\right.\\
&\qquad\left.\frac{\eta(t)\tilde{f}_t(0)}{4B\overline{S}_+^{\rm hf}(t)}\left(\dot{\overline{S}}_+^{\rm hf}(t)+\frac{\overline{\sigma}_{0+}^2}{\overline{\sigma}_{0-}^2}\dot{\overline{S}}_-^{\rm hf}(t)\right)\right\}\\
\left(\cos^2\overline{\chi}\dot{\tilde{\Sigma}}_{2k+1}^{\beta}-\sin^2\overline{\chi}\dot{\tilde{\Sigma}}_{2k+1}^{\alpha}\right) &= \frac{B_x^2B_z^2}{2B^5}\eta(t)\left[\tilde{f}_t(0)\left(\sigma_{0-}^2\dot{\overline{S}}_+^{\rm hf}(t)+\frac{1}{2}\overline{\sigma}_{0+}^2\dot{S}_-^{\rm hf}(t)\right)+\dot{\tilde{f}}_t(0)\overline{\sigma}_{0+}^2S_-^{\rm hf}(t)\right]\\
\left(\dot{\tilde{\Sigma}}_{2k+1}^{\gamma}+\dot{\tilde{\Sigma}}_{2k+1}^{\delta}+\dot{\tilde{\Sigma}}_{2k+1}^{\epsilon}\right) &= \frac{B_x^2B_z^2}{2B^5}\eta(t)\sigma_{0-}^2\left[\frac{2\tilde{f}_t(0)}{B^2}\eta(t)\overline{\sigma}_{0+}^2S_-^{\rm hf}(t)\dot{\overline{S}}_+^{\rm hf}(t)-\frac{1}{2}\tilde{f}_t(0)\dot{S}_-^{\rm hf}(t)-\dot{\tilde{f}}_t(0)S_-^{\rm hf}(t)\right]\\
\left(\dot{\tilde{\Sigma}}_{2k+1}^{\gamma}-\dot{\tilde{\Sigma}}_{2k+1}^{\delta}\right) &= \frac{B_x^2B_z^2}{2B^5}\eta(t)\left[\frac{\tilde{f}_t(0)}{B^2}\eta(t)\sigma_{0-}^2S_-^{\rm hf}(t)\left(\dot{\overline{S}}_+^{\rm hf}(t)\overline{\sigma}_{0-}^2+\dot{\overline{S}}_-^{\rm hf}(t)\overline{\sigma}_{0+}^2\right)-\right.\\
&\qquad\left.\frac{\tilde{f}_t(0)}{4}\left(\sigma_{0-}^2\dot{S}_+^{\rm hf}(t)+\sigma_{0+}^2\dot{S}_-^{\rm hf}(t)\right)-\frac{\dot{\tilde{f}}_t(0)}{2}\left(\sigma_{0-}^2S_+^{\rm hf}(t)+\sigma_{0+}^2S_-^{\rm hf}(t)\right)\right],
\end{aligned}\tag{IV.19}$$

and for even sums (start at $k=2$)

$$\begin{aligned}
\dot{\Sigma}_{2k}^{\gamma}+\dot{\Sigma}_{2k}^{\delta}+\dot{\Sigma}_{2k}^{\epsilon} &= \frac{\eta(t)}{2B^2}\dot{\overline{S}}_+^{\rm hf}(t)\overline{\sigma}_{0+}^2\\
\dot{\Sigma}_{2k}^{\gamma}-\dot{\Sigma}_{2k}^{\delta} &= \frac{\eta(t)}{4B^2}\left[\dot{\overline{S}}_+^{\rm hf}(t)\overline{\sigma}_{0-}^2+\dot{\overline{S}}_-^{\rm hf}(t)\overline{\sigma}_{0+}^2\right]\\
\cos^2\overline{\chi}\dot{\tilde{\Sigma}}_{2k}^{\beta}-\sin^2\overline{\chi}\dot{\tilde{\Sigma}}_{2k}^{\alpha} &= \frac{\left(B_xB_z\right)^2}{2B^6}\eta(t)\overline{\sigma}_{0+}^2\left[\frac{\partial\tilde{f}_t^2(0)}{\partial t}\sigma_{0-}^2\overline{S}_+^{\rm hf}(t)+\frac{1}{2}\frac{d}{dt}\left(\overline{S}_+^{\rm hf}(t)S_-^{\rm hf}(t)\right)\right]\\
\dot{\tilde{\Sigma}}_{2k}^{\gamma}+\dot{\tilde{\Sigma}}_{2k}^{\delta}+\dot{\tilde{\Sigma}}_{2k}^{\epsilon} &= \frac{\left(B_xB_z\right)^2}{2B^6}\eta(t)\left[\tilde{f}_t^2(0)\sigma_{0-}^4\dot{\overline{S}}_+^{\rm hf}(t)\left(\frac{\eta(t)}{B^2}\overline{\sigma}_{0+}^2\overline{S}_+^{\rm hf}(t)-1\right)+\frac{\eta(t)}{B^2}\overline{\sigma}_{0+}^4\left[S_-^{\rm hf}(t)\right]^2\dot{\overline{S}}_+^{\rm hf}(t)-\overline{\sigma}_{0+}^2S_-^{\rm hf}(t)\dot{S}_-^{\rm hf}(t)\right]\\
\dot{\tilde{\Sigma}}_{2k}^{\gamma}-\dot{\tilde{\Sigma}}_{2k}^{\delta} &= \frac{\left(B_xB_z\right)^2}{4B^6}\eta(t)\left\{\frac{\eta(t)}{B^2}\left[\tilde{f}_t^2(0)\sigma_{0-}^4\overline{S}_+^{\rm hf}(t)+\overline{\sigma}_{0+}^2\left[S_-^{\rm hf}(t)\right]^2\right]\left(\dot{\overline{S}}_+^{\rm hf}(t)\overline{\sigma}_{0-}^2+\dot{\overline{S}}_-^{\rm hf}(t)\overline{\sigma}_{0+}^2\right)-\right.\\
&\qquad\left.\tilde{f}_t^2(0)\sigma_{0-}^2\left(\sigma_{0-}^2\dot{\overline{S}}_-^{\rm hf}(t)+\sigma_{0+}^2\dot{\overline{S}}_+^{\rm hf}(t)\right)-\frac{\overline{\sigma}_{0+}^2}{2}\frac{d}{dt}\left[S_-^{\rm hf}(t)S_+^{\rm hf}(t)\right]-\frac{\overline{\sigma}_{0-}^2}{2}\frac{d}{dt}\left[S_-^{\rm hf}(t)\right]^2\right\}.
\end{aligned}\tag{IV.20}$$

In Eqs. (IV.19) and (IV.20), $\eta(t)$ is defined in Eq. (17) in the main text. Notice that since $\tilde{f}_t(0)=0$ for any balanced DD pulse sequence, all time derivatives of odd cumulant sums vanish, except for FID. In this case, the above sums are found by

substituting $S_l^{\rm hf}(t)\to\sigma_{0l}^2t^2$ and dividing all sums except the odd linked ones by 2. We find for the odd sums:

$$\begin{aligned}
\left(\dot\Sigma_{2k+1}^{\gamma,\rm FID}+\dot\Sigma_{2k+1}^{\delta,\rm FID}+\dot\Sigma_{2k+1}^{\epsilon,\rm FID}\right)&=\frac{\overline{\sigma}_{0+}^2\eta_{\rm FID}(t)}{2B}\\
\left(\dot\Sigma_{2k+1}^{\gamma,\rm FID}-\dot\Sigma_{2k+1}^{\delta,\rm FID}\right)&=\frac{\overline{\sigma}_{0-}^2\eta_{\rm FID}(t)}{2B}\\
\left(\cos^2\overline{\chi}\dot{\tilde\Sigma}_{2k+1}^{\beta,\rm FID}-\sin^2\overline{\chi}\dot{\tilde\Sigma}_{2k+1}^{\alpha,\rm FID}\right)&=\frac{2B_x^2B_z^2}{B^5}\eta_{\rm FID}(t)\overline{\sigma}_{0+}^2\sigma_{0-}^2t^2\\
\left(\dot{\tilde\Sigma}_{2k+1}^{\gamma,\rm FID}+\dot{\tilde\Sigma}_{2k+1}^{\delta,\rm FID}+\dot{\tilde\Sigma}_{2k+1}^{\epsilon,\rm FID}\right)&=\frac{B_x^2B_z^2}{B^5}\eta_{\rm FID}(t)\sigma_{0-}^4t^2\left(\frac{2\eta_{\rm FID}(t)}{B^2}\overline{\sigma}_{0+}^4t^2-1\right)\\
\left(\dot{\tilde\Sigma}_{2k+1}^{\gamma,\rm FID}-\dot{\tilde\Sigma}_{2k+1}^{\delta,\rm FID}\right)&=\frac{B_x^2B_z^2}{B^5}\eta_{\rm FID}(t)\sigma_{0+}^2\sigma_{0-}^2t^2\left(\frac{2\eta_{\rm FID}(t)\sigma_{0-}^2}{B^2\sigma_{0+}^2}\overline{\sigma}_{0+}^2\overline{\sigma}_{0-}^2t^2-1\right),
\end{aligned}\tag{IV.21}$$

and for even sums (starting at $k=2$)

$$\begin{aligned}
\dot\Sigma_{2k}^{\gamma,\rm FID}+\dot\Sigma_{2k}^{\delta,\rm FID}+\dot\Sigma_{2k}^{\epsilon,\rm FID}&=\frac{\eta_{\rm FID}(t)}{B^2}\overline{\sigma}_{0+}^4t\\
\dot\Sigma_{2k}^{\gamma,\rm FID}-\dot\Sigma_{2k}^{\delta,\rm FID}&=\frac{\eta_{\rm FID}(t)}{B^2}\overline{\sigma}_{0+}^2\overline{\sigma}_{0-}^2t\\
\cos^2\overline{\chi}\dot{\tilde\Sigma}_{2k}^{\beta,\rm FID}-\sin^2\overline{\chi}\dot{\tilde\Sigma}_{2k}^{\alpha,\rm FID}&=2\left(\frac{B_xB_z}{B^3}\right)^2\eta_{\rm FID}(t)\overline{\sigma}_{0+}^4\sigma_{0-}^2t^3\\
\dot{\tilde\Sigma}_{2k}^{\gamma,\rm FID}+\dot{\tilde\Sigma}_{2k}^{\delta,\rm FID}+\dot{\tilde\Sigma}_{2k}^{\epsilon,\rm FID}&=2\left(\frac{B_xB_z}{B^3}\right)^2\eta_{\rm FID}(t)\sigma_{0-}^4\overline{\sigma}_{0+}^2t^3\left(\frac{\eta_{\rm FID}(t)}{B^2}\overline{\sigma}_{0+}^4t^2-1\right)\\
\dot{\tilde\Sigma}_{2k}^{\gamma,\rm FID}-\dot{\tilde\Sigma}_{2k}^{\delta,\rm FID}&=\left(\frac{B_xB_z}{B^3}\right)^2\eta_{\rm FID}(t)\sigma_{0-}^2t^3\left[\frac{2\eta_{\rm FID}(t)}{B^2}\sigma_{0-}^2\overline{\sigma}_{0-}^2\overline{\sigma}_{0+}^4t^2-\left(\overline{\sigma}_{0+}^2\sigma_{0+}^2+\overline{\sigma}_{0-}^2\sigma_{0-}^2\right)\right].
\end{aligned}\tag{IV.22}$$

V. SUBLEADING CONTRIBUTION FOR ODD LINKED TERMS FOR BALANCED SEQUENCES

For any balanced pulse sequence, both linked and semi-linked diagrams and their derivatives vanish to leading order in σ_{0l}. Here we calculate the subleading contribution for the odd linked diagrams (similar contribution to the semi-linked terms is yet an order of magnitude smaller and is thus not considered).

The leading contribution in the odd linked terms, Eq. (IV.4), was evaluated by alternating $k+1$ low-frequency σ_{0l}^2 factors with k high-frequency noise correlators, so as to obtain a maximal power of σ_{0l}^2 factors. In the subleading contribution we consider k σ_{0l}^2 factors alternating with $k+1$ high-frequency correlators. The resulting term is:

$$\begin{aligned}
R_{2k+1}^{\rm sub}(t_\gamma,t_\delta,t_\epsilon)=\frac{i(-1)^{k+1}}{2B^{2k+1}}\Bigg\{&\underbrace{F_0(t_\gamma,t_\delta)\frac{\left[s\sigma_1t_\gamma,t_\delta\right]^{k-1}}{2k+1}}_{m=0\ (k\geq1)}+\frac{1}{2}\underbrace{F_1(t_\gamma,t_\delta,t_\epsilon)\left(\frac{B_xB_z}{B^2}\right)^2\left[s\sigma_1t_\gamma,t_\delta\right]^{k-2}}_{m=1\ (k\geq2)}+\\
&\underbrace{\frac{1}{4}F_2(t_\gamma,t_\delta,t_\epsilon)\left(\frac{B_xB_z}{B^2}\right)^4\sum_{m=2}^{k}\frac{1}{2k+1-m}\binom{2k+1-m}{m}\left[s\sigma_1(t_\gamma,t_\delta)\right]^{k-m-1}\left[s\sigma_2(t_\gamma,t_\delta,t_\epsilon)\right]^{m-2}}_{k\geq3}\Bigg\},
\end{aligned}\tag{V.1}$$

where:

$$
\begin{aligned}
F_0(t_\gamma,t_\delta) &= \sin^2\overline{\chi}S_{3z}^{\mathrm{hf},\gamma}+\cos^2\overline{\chi}S_{3x}^{\mathrm{hf},\delta}\\
F_1(t_\gamma,t_\delta,t_\epsilon) &= \sin^2\overline{\chi}\left[S_z^{\mathrm{hf}}(t_\gamma,t_\epsilon)S_{3+}^{\mathrm{hf},\epsilon}-\frac{1}{2}\left(S_z^{\mathrm{hf}}(t_\gamma,t_\gamma)S_{3+}^{\mathrm{hf},\delta}+S_z^{\mathrm{hf}}(t_\gamma,t_\delta)S_{3+}^{\mathrm{hf},\gamma}\right)\right]+\\
&\quad \cos^2\overline{\chi}\left[S_x^{\mathrm{hf}}(t_\delta,t_\epsilon)S_{3+}^{\mathrm{hf},\epsilon}-\frac{1}{2}\left(S_x^{\mathrm{hf}}(t_\delta,t_\gamma)S_{3+}^{\mathrm{hf},\delta}+S_x^{\mathrm{hf}}(t_\delta,t_\delta)S_{3+}^{\mathrm{hf},\gamma}\right)\right]\\
F_2(t_\gamma,t_\delta,t_\epsilon) &= \left(\sin^2\overline{\chi}S_z^{\mathrm{hf}}(t_\gamma,t_\epsilon)+\cos^2\overline{\chi}S_x^{\mathrm{hf}}(t_\delta,t_\epsilon)\right)\left[S_{2+}^{\mathrm{hf}}(t_\delta,t_\epsilon)S_{3+}^{\mathrm{hf},\epsilon}-\frac{1}{2}\left(S_{2+}^{\mathrm{hf}}(t_\epsilon,t_\gamma)S_{3+}^{\mathrm{hf},\gamma}+S_{2+}^{\mathrm{hf}}(t_\epsilon,t_\delta)S_{3+}^{\mathrm{hf},\gamma}\right)\right]-\\
&\quad \frac{1}{2}\left(\sin^2\overline{\chi}S_z^{\mathrm{hf}}(t_\gamma,t_\gamma)+\cos^2\overline{\chi}S_x^{\mathrm{hf}}(t_\delta,t_\gamma)\right)\left[S_{2+}^{\mathrm{hf}}(t_\delta,t_\epsilon)S_{3+}^{\mathrm{hf},\epsilon}-\frac{1}{2}\left(S_{2+}^{\mathrm{hf}}(t_\delta,t_\gamma)S_{3+}^{\mathrm{hf},\delta}+S_{2+}^{\mathrm{hf}}(t_\delta,t_\delta)S_{3+}^{\mathrm{hf},\gamma}\right)\right]-\\
&\quad \frac{1}{2}\left(\sin^2\overline{\chi}S_z^{\mathrm{hf}}(t_\gamma,t_\delta)+\cos^2\overline{\chi}S_x^{\mathrm{hf}}(t_\delta,t_\delta)\right)\left[S_{2+}^{\mathrm{hf}}(t_\gamma,t_\epsilon)S_{3+}^{\mathrm{hf},\epsilon}-\frac{1}{2}\left(S_{2+}^{\mathrm{hf}}(t_\gamma,t_\gamma)S_{3+}^{\mathrm{hf},\delta}+S_{2+}^{\mathrm{hf}}(t_\gamma,t_\delta)S_{3+}^{\mathrm{hf},\gamma}\right)\right], \qquad \text{(V.2)}
\end{aligned}
$$

and we have defined:

$$
\begin{aligned}
S_{3l}^{\mathrm{hf},i}(t_\gamma,t_\delta,t_i) &= \int dt_1dt_2dt_3\left[\sin^2\overline{\chi}f_{t_\gamma}(t_1)S_z^{\mathrm{hf}}(t_{12})+\cos^2\overline{\chi}f_{t_\delta}(t_1)S_x^{\mathrm{hf}}(t_{12})\right]\times\\
&\qquad \left[\sin^2\overline{\chi}f_{t_\gamma}(t_2)\sigma_{0z}^2+\cos^2\overline{\chi}f_{t_\delta}(t_2)\sigma_{0x}^2\right]f_{t_i}(t_3)S_l^{\mathrm{hf}}(t_{31})\\
S_{3+}^{\mathrm{hf},i}(t_\gamma,t_\delta,t_i) &= S_{3z}^{\mathrm{hf},i}\sigma_{0x}^2+S_{3x}^{\mathrm{hf},i}\sigma_{0z}^2\\
S_{2+}^{\mathrm{hf}}(t_i,t_j) &= S_z^{\mathrm{hf}}(t_i,t_j)\sigma_{0x}^2+S_x^{\mathrm{hf}}(t_i,t_j)\sigma_{0z}^2. \qquad \text{(V.3)}
\end{aligned}
$$

From these formulas, we calculate the subleading contributions to the odd linked cumulant sum, and its time derivatives as:

$$
\Sigma_{2k+1}=\frac{\overline{S}_{3+}^{\mathrm{hf}}(t)\rho(t)}{\overline{\sigma}_{0+}^2\overline{S}_{+}^{\mathrm{hf}}(t)}, \qquad \text{(V.4)}
$$

and

$$
\begin{aligned}
\left(\dot{\Sigma}_{2k+1}^{\gamma}+\dot{\Sigma}_{2k+1}^{\delta}+\dot{\Sigma}_{2k+1}^{\epsilon}\right) &= \frac{1}{2\overline{\sigma}_{0+}^2\overline{S}_{+}^{\mathrm{hf}}(t)}\left\{\left(\frac{\cos\overline{\chi}}{B_z}-\rho(t)\right)\left[\frac{\dot{\overline{S}}_{+}^{\mathrm{hf}}(t)}{\overline{S}_{+}^{\mathrm{hf}}(t)}\overline{S}_{3+}^{\mathrm{hf}}(t)+\dot{\overline{S}}_{3+}^{\mathrm{hf}}(t)\right]+\frac{1}{2}\left(\frac{B_z\eta(t)}{\cos\overline{\chi}}-\rho(t)\right)\frac{\dot{\overline{S}}_{+}^{\mathrm{hf}}(t)}{\overline{S}_{+}^{\mathrm{hf}}(t)}\overline{S}_{3+}^{\mathrm{hf}}(t)\right\}\\
\left(\dot{\Sigma}_{2k+1}^{\gamma}-\dot{\Sigma}_{2k+1}^{\delta}\right) &= \frac{\overline{S}_{3+}^{\mathrm{hf}}(t)}{2\overline{\sigma}_{0+}^2\overline{S}_{+}^{\mathrm{hf}}(t)}\left\{\left[\frac{\cos\overline{\chi}}{B_z}+\frac{B_z\eta(t)}{2\cos\overline{\chi}}-\frac{3}{2}\rho(t)\right]\left[\frac{\dot{\overline{S}}_{+}^{\mathrm{hf}}(t)\overline{\sigma}_{0-}^2+\dot{\overline{S}}_{-}^{\mathrm{hf}}(t)\overline{\sigma}_{0+}^2}{2\dot{\overline{S}}_{+}^{\mathrm{hf}}(t)\overline{\sigma}_{0+}^2}\right]+\frac{\dot{\overline{S}}_{3-}^{\mathrm{hf}}(t)}{\overline{S}_{3+}^{\mathrm{hf}}(t)}\left(\rho(t)-\frac{\cos\overline{\chi}}{B_z}\right)\right\}. \qquad \text{(V.5)}
\end{aligned}
$$

In the above formulas we have defined

$$
\overline{S}_{3+}^{\mathrm{hf}}(t)\equiv\sin^2\overline{\chi}S_{3z}^{\mathrm{hf}}(t)+\cos^2\overline{\chi}S_{3x}^{\mathrm{hf}}(t), \qquad \text{(V.6)}
$$

and

$$
\rho(t)\equiv\frac{\arctan\left(\frac{1}{B}\sqrt{\overline{\sigma}_{0+}^2\overline{S}_{+}^{\mathrm{hf}}(t)}\right)}{\sqrt{\overline{\sigma}_{0+}^2\overline{S}_{+}^{\mathrm{hf}}(t)}}, \qquad \text{(V.7)}
$$

and the explicit spectral integrations read:

$$
S_{3l}^{\mathrm{hf}}(t)=\int_0^\infty\int_0^\infty\frac{d\omega_1d\omega_2}{2\pi^2}\overline{\sigma}_{0+}^2\tilde{\overline{S}}_{+}^{\mathrm{hf}}(\omega_1)\tilde{S}_l^{\mathrm{hf}}(\omega_2)\left[\tilde{f}_t(\omega_1-\omega_2)\tilde{f}_t(-\omega_1)\tilde{f}_t(\omega_2)+h.c.\right], \qquad \text{(V.8)}
$$

and

$$\dot{\overline{S}}^{\rm hf}_{3+}(t) = \sin^2\overline{\chi}\left(\frac{\partial S^{{\rm hf},\gamma}_{3z}}{\partial t_\gamma}+\frac{\partial S^{{\rm hf},\gamma}_{3z}}{\partial t_\delta}\right)\Bigg|_{t_i\to t}+\cos^2\overline{\chi}\left(\frac{\partial S^{{\rm hf},\delta}_{3x}}{\partial t_\gamma}+\frac{\partial S^{{\rm hf},\delta}_{3x}}{\partial t_\delta}\right)\Bigg|_{t_i\to t}=$$
$$\int_0^\infty\int_0^\infty\frac{d\omega_1 d\omega_2}{2\pi^2}\overline{\sigma}^2_{0+}\tilde{\overline{S}}^{\rm hf}_+(\omega_1)\tilde{\overline{S}}^{\rm hf}_+(\omega_2)\left[\frac{\partial}{\partial t}\left(\tilde{f}_t(\omega_1-\omega_2)\tilde{f}_t(-\omega_1)\tilde{f}_t(\omega_2)\right)+h.c.\right]$$
$$\dot{\overline{S}}^{\rm hf}_{3-}(t) = \sin^2\overline{\chi}\left(\frac{\partial S^{{\rm hf},\gamma}_{3z}}{\partial t_\gamma}-\frac{\partial C^{{\rm hf},\gamma}_{3z}}{\partial t_\delta}\right)\Bigg|_{t_i\to t}+\cos^2\overline{\chi}\left(\frac{\partial S^{{\rm hf},\delta}_{3x}}{\partial t_\gamma}-\frac{\partial S^{{\rm hf},\delta}_{3x}}{\partial t_\delta}\right)\Bigg|_{t_i\to t}=\int_0^\infty\int_0^\infty\frac{d\omega_1 d\omega_2}{2\pi^2}\overline{\sigma}^2_{0+}\times$$
$$\left[\tilde{\overline{S}}^{\rm hf}_-(\omega_1)\tilde{\overline{S}}^{\rm hf}_+(\omega_2)\frac{\partial}{\partial t}\left(\tilde{f}_t(\omega_1-\omega_2)\tilde{f}_t(-\omega_1)\right)\tilde{f}_t(\omega_2)+\tilde{\overline{S}}^{\rm hf}_+(\omega_1)\tilde{\overline{S}}^{\rm hf}_-(\omega_2)\tilde{f}_t(\omega_1-\omega_2)\tilde{f}_t(-\omega_1)\dot{\tilde{f}}_t(\omega_2)+h.c.\right] \quad \text{(V.9)}$$

with

$$\tilde{\overline{S}}^{\rm hf}_\pm(\omega)\equiv\sin^2\overline{\chi}\tilde{S}^{\rm hf}_z(\omega)+\cos^2\overline{\chi}\tilde{S}^{\rm hf}_x(\omega). \quad \text{(V.10)}$$

We note that $\tilde{f}_t(\omega_1-\omega_2)\tilde{f}_t(-\omega_1)\tilde{f}_t(\omega_2)$ in Eq. (V.8) is pure imaginary for odd number of DD pulses thus these subleading contributions to $R_{2k+1}(t)$ and its time derivatives vanish in this case.

[1] E. Barnes, M. S. Rudner, F. Martins, F. K. Malinowski, C. M. Marcus, and F. Kuemmeth, Filter function formalism beyond pure dephasing and non-markovian noise in singlet-triplet qubits, Phys. Rev. B **93**, 121407(R) (2016).

[2] F. K. Malinowski, F. Martins, Ł. Cywiński, M. S. Rudner, P. D. Nissen, S. Fallahi, G. C. Gardner, M. J. Manfra, C. M. Marcus, and F. Kuemmeth, Spectrum of the nuclear environment for gaas spin qubits, Phys. Rev. Lett. **118**, 177702 (2017).

[3] F. Martins, F. K. Malinowski, P. D. Nissen, E. Barnes, S. Fallahi, G. C. Gardner, M. J. Manfra, C. M. Marcus, and F. Kuemmeth, Noise suppression using symmetric exchange gates in spin qubits, Phys. Rev. Lett. **116**, 116801 (2016).